University of Southampton

Faculty of Engineering, Science & Mathematics

School of Physics and Astronomy

Studies of the low frequency dielectric constants and conductance of two molecular systems; carbon nanotubes and polyaromatic molecular wires.

By

Daniel Walker

Thesis for the degree of Master of Philosophy

June 2008

Contents

Acknowledgments

I would like to thank all the individuals who had an input into this project including all those I worked with, particularly Dr D. C. Smith's post graduate and post doctoral researchers. I must thank Dr D. C. Smith, my supervisor, for having many of the ideas associated with both parts of the project, running the first part and massive input and support in the writing of the thesis. I thank Dr N. Green for setting up and supervising the second part of the project and Dr I. Nandhakumar for ideas and solutions to some of the problems we encountered. I should also thank Dr C. E. Gardner for support and direction whilst working with me on the first project in this thesis and Dr M. A. Ghanem for completing much of the work that Dr Gardner and I continued.

Abstract

This thesis deals with two projects on the electronic properties of molecular systems. Presented first is an experiment designed to characterize the direct current charge transport characteristics of polyaromatic molecular wires, specifically oligo(phenylene ethynylene) or a five benzene ring variant 1,4-bis(2-(4-(2-(4-thioacetylphenyl)ethynyl)phenyl)ethynyl)-2,5-didodecylbenzene. The techniques and methods used to make and contact these molecular wires are given and followed up a discussion of the results and conclusions. The molecular wires were contacted by adsorbing them into a prefabricated device. A gold wire, approximately 100nm in diameter and 10μm in length was grown electrochemically with a self assembled monolayer spacer grown into the wire at 5 μm. These gold wires were contacted photolithographically resulting in a device that could be electrically contacted allowing measurement of the material in the middle of the wire. The spacer could then be removed by volatilizing away the self assembled monolayer used leaving a contacted gold wire with a nanometer scale gap at its centre. The molecular wires could then be adsorbed across this gap allowing a measurement of their properties. Using the test bed developed a measurement of resistance of oligo(phenylene ethynylene) of 44GΩ in close agreement with other groups contact atomic force microscopy methods.

The second part to this thesis details the measurement of carbon nanotubes suspended in 1,2 - dichlorobenzene using impedance spectroscopy. A brief account of the theory used to understand the observed effects is presented followed by a description of the methods and results. The nanotubes were suspended in the 1,2 – dichlorobenzene at a maximum concentration of 90mg/L without a surfactant and measured across a frequency range from 10^7Hz to 1Hz at varying electric field strengths. This was performed in a cell that was very large compared to the nanotubes themselves and had plates with a large surface area compared to their separation to keep the field as uniform as possible. The frequency spectra were run at increasing field strengths and a drop in the real part of the impedance of the solution between the plates from $2x10^7\Omega$ to $1x10^5\Omega$ was observed as the electric field strength was increased. This drop in impedance did not continue as the field strength was increased further but saturated at $1x10^5\Omega$, with further decreases unobservable at the electric field strengths available to us. However it was found that the rate at which this threshold was reached depended strongly on the electric field strength and the concentration of the nanotubes in the suspension. Further work detailed in this projects show that this change in impedance is semi-permanent with no measurable decay to the original impedance observable over 8 hours. The system can be made to return towards is original state by agitation and the project shows that the more vigorous the agitation the closer to the original value of the impedance the solution becomes. This leads to the projects conclusion that chain formation or aggregation is the ultimate cause of the observed decrease in impedance although the details of the mechanism that causes this decrease in impedance remain unclear.

Introduction

This project is written in two parts in such a way that they may be read separately. Whilst there are similarities between the parts in that they are in the same area of science there are also many differences as the experimental techniques used are different.

The first part of this project details the attempts to characterize the electronic properties of molecular wires containing three or five benzene rings. This work is laid out first detailing the aims and reasons behind the project. There follows some introduction to the theory of molecular conduction before the experimental techniques used are described. There is then a detailed discussion into the problems that were encountered with these techniques and how these problems were solved or their effect minimised before the results are presented and conclusions drawn. This work is covered in the paper titled Development of a Nanowire-Based Test Bed Device for Molecular Electronics Applications[1].

The second part to this project is set out in a similar way to the first part with an introduction to the ideas, aims and theory. Following this are the details of the experimental techniques used and the results which lead on to a detailed discussion of these results and the conclusions that were reached. The ideas for experiments in this part of the project which can be attributed to Dr N. Green, Dr D. C. Smith and Dr I. Nandhakumar were originally to discover an ideal set of parameters for frequency and field strength of an applied alternating current electric field to aid in their separation by dielectrophoresis. This second part of the project starts on page 36.

Part 1 - Measurement of the D.C. Characteristics of Molecular Wires Using a Gapped Nanowire Junctions.

Introduction

For molecular electronics to be integrated successfully into working devices an understanding of how molecules behave when a voltage is applied to them is vital. It is also critical that a reliable metal – molecule – metal junction can be fabricated to include the molecules into electronic circuits. This project uses lithographically contacted gold wires with molecular scale gaps to measure current voltage characteristics of self assembled monolayers (SAMs) and molecules.

This is not the only method for measuring the electronic properties of molecules but it is novel and has some distinct advantages over existing methods as will be discussed below. These methods can be broadly divided into three categories which I will call contact methods, where one metallic object coated with a SAM is brought very close to or into contact with another, scanning probe microscopy methods, where an atomic force microscope (AFM) or scanning tunnelling microscope (STM) is used to measure molecular properties and fabricated methods, where the SAM is grown into a wire or built into a device. A more in depth review of all the methods mentioned including schematic diagrams is given in a review by Mantooth and Weiss[2].

Contact methods include the Mercury Drop Junction, Nanoparticle Bridged Gap and Crossed Wires methods. In the Mercury Drop Method a bead of mercury is brought into contact with a metallic film in a thiol solution. The thiol will have formed SAMs on both the silver film and the mercury drop creating a metal – double SAM – metal junction[3]. There can be different thiols in each solution and the thiols on the mercury drop and the metal film need not be the same. This is described as an experimentally simple method for measuring current flow across SAMs and overcomes the problem of reproducibly contacting both ends of any molecule. Because of its simplicity it allows many combinations of metals and SAMs to be studied. Also, although it is not explicitly mentioned, the surface tension of the mercury stops it creeping down defects in the SAM reducing the chance of creating filaments of metal through the SAM which can be a major problem for other techniques. This method is complicated by the fact that there are two SAMs in the gap and in fact has been modified by Selzer et al to have a mercury – SAM – semiconductor junction to make the analysis simpler[4,5]. Both of these methods are limited by not knowing how many molecules form the interface between the metals and by not being able to measure single or very small numbers of molecules due to the large contact areas of the electrodes. Finally these methods could never be included into a working device.

The following methods could both be included in working devices. They are the Bridged Gap method by Amlani[6] et al and the Crossed Wire method by Kushmerick[7]et al. In the bridged gap method metal contacts are created by a combination of photolithography and electron beam lithography with a gap of 40 – 100 nm wide. This is then soaked in a SAM solution which coats the metals. Nanoparticles are introduced and an A.C. electric field applied to trap these nanoparticles between the gap. Although this is a complicated junction it has been shown that it behaves as two resonant tunnelling diodes in series[8] and allows measurement of this system, which no other method does. Again this method is limited by only being able to measure complete SAMs not single or small numbers of molecules and similar to the mercury drop it would be very difficult to know how many molecules are between the contacts and the nanoparticle.

The crossed wire method involves treating one of the wires with a thiol to create a SAM and aligning the second wire perpendicularly across it. The method of doing this described by Gregory[9] is complicated requiring liquid helium temperatures and magnetic fields. However it does allow small numbers of molecules to be measured as the contact area between the wires is small and well defined. If a simpler technique for crossing the wires could be found then this geometry is ideal for inclusion in electronic circuits as once it is assembled it is robust with the molecular film serving as both the tunnelling barrier and a glue to keep the wires together[9].

The second set of measurement techniques used are the scanning probe microscopy methods. An overview of these is given by Samori and Rabe[10]. This includes the use of a scanning tunnelling microscope (STM); perhaps the most widely used technique. Many groups use the STM because it can image and measure very small numbers of and even individual molecules with a certainty that other methods do not provide[11]. The most common of the STM methods is to take a SAM and insert the molecule of interest into a defect site[12]. This works as a defect site on the SAM will expose the metal coated surface of the substrate and the molecules are picked to have end groups which are chemically attracted to the metal surface. A common example is a gold surface and thio-acetate end group where the sulphur is strongly attracted to the gold. The STM is then used in constant current mode to image the surface[13] allowing the molecules to be seen. The tip is then returned to the position of a molecule and the current measured as a function of the voltage[2, 14]. Another method employed by Haiss[11] is to cover a gold surface with a low concentration of molecules, find them with the STM, then take the tip close to the surface such that one end of the molecule binds to the STM tip, the other remaining bound to the surface. The tip is then retracted pulling the molecule into a wire between the surface and the tip whilst the current is recorded. When the tip gets too far from the surface the wire breaks and a sharp drop in current is observed.

Unlike other methods the STM can be used to measure single molecules with certainty and Haiss has published results showing the attachment and detachment of single molecules in the form of current jumps in current as a function of time measurements made with an STM[15]. This ability allows observation of these molecules uninterrupted over time and had allowed groups to measure a reversible change in electron transport for a period of tens of minutes measured as a change in apparent height of the molecules showing they have more than one stable conduction state[2, 14]. It has been found that the surrounding material plays an important role in the switching behaviour of molecules so it is likely the change is due to a change in orientation or position of the molecule.

However STM is by no means the perfect method for measuring single molecule electronics. The data obtained from the STM in its raw state is complicated by the tunnelling barrier used to control the STM feedback loop and modelling is required to determine which components of the current – voltage characteristics are due to the molecule – tip tunnelling and which are due to tunnelling through the molecule. Work has been done on this and it has been shown that the double barrier tunnel junction can be represented as pairs of resistors and capacitors in parallel[16]. Also it is questionable in the case of a molecule in the defect site of a SAM whether all the electron transport is through the molecule or whether there is a significant contribution from the surrounding material. A further issue with this is that the molecules are at defect sites so it is not possible to know the exact geometry around the site or of the substrate the molecule is attached to. The pull back method of Haiss does not have these issues

but here it is not certain that the very end of the molecule bonds to the very end of the tip. This could lead to tunnelling from the tip to a point half way down the molecule making the results very hard to interpret and leading to false impressions of the resistance.

Finally STM techniques will never be included in a working molecular electronics device, but despite these uncertainties it is probably the best method available for measuring the resistance of single molecules. The second SPM technique is conducting atomic force microscopy (cAFM). Here a metal coated AFM tip is brought into contact with the surface coated with a SAM, the metal coated substrate – SAM – metal tip then behaves as a single tunnelling junction with an exponential resistance increase with SAM thickness[17]. cAFM cannot be used to directly measure single molecules as the area of the tip is too large and any attempt would result in also measuring the surrounding material, however Lindsay et al have managed to measure single molecule resistance by treating a surface, which has the molecules to be measured inserted into SAM defects, with nanoparticles which bond to the exposed ends of the molecules[18]. These can then be contacted by the cAFM tip. Even with this method it is by no means certain that only one molecule contributes to the conduction and Lindsay mentions that if more than one are attached, each contribute equally to the conduction. So for this method you need to know how many molecules are attached to the nanoparticle which is not easy.

One unique property of using an AFM is that it allows the application of force to the molecules being studied and this has been used to show that the conductance of alkanethiol does depend on the stress applied and that the longer the chain the less sensitive it is[19]. Conversely other molecules such as 1-8-octanedithiol are not at all sensitive to force applied.

Problems with cAFM are principally that it can be hard to know how many molecules are contacted and that like STM it will never be used in a working device. It is also hard to know how much weight to attach to cAFM results, for example the measured resistance of OPE by STM is $1.7 \pm 0.4G\Omega$ and $1.9 \pm 0.5G\Omega$ in film form[20] whereas cAFM has measured the resistance of single OPE molecules as $51 \pm 18G\Omega$[21].

The final set of systems in use are the fabricated devices. These include break junctions, nanopores and gapped wires. Break junctions were used in some of the first molecular electronics measurements and work by using a piezoelectric actuator to stress a notched wire. This wire will fracture at the notch leaving a gap the width of which can be controlled by the actuator. The molecule of interest can then added and the ends of the wire bought back towards each other until one molecule bridges the gap[22, 23]. Alternatively once the break has been made the gap can be closed by electro-migration where a voltage is applied across the gap. The atoms at the ends then creep towards each other. This is continued until a tunnelling current is observed indicating a small gap[24]. The molecules are then added and the properties measured.

Although this method does not sound complicated it has to be performed in a carefully controlled environment to stop chemical reactions at the tips producing unwanted compounds. Also it happens that several stable junctions with the same molecule may produce different results which are attributed to changes in the geometry of the junction[24]. It is hard in a lot of the other methods to know exactly how any molecules are positioned in relation to the surroundings, but in the break junction it is close to impossible to know the nature of the junction making analysis of results very difficult. This

method is also only suited to rigid molecules so longer more flexible molecules cannot be measured reliably since they further complicate the junction.

The nanopores device, made by the same group who did the break junction method, can be used to measure small numbers of organic molecules in self assembled monolayers[25]. These devices are made by electron beam lithography and plasma etching to form a small dish shape in silicon with a small hole in the bottom. The dish is then filled with gold to act as the top contact. The device is then immersed in a solution containing the molecules of interest and a SAM allowed to form in the hole. The bottom surface then has gold evaporated onto it creating a SAM sandwich. The device can then be contacted up to measure electronic properties of the SAM which can be as small as a few thousand molecules. The advantage of such a device is that it could be incorporated into circuits and it has been proposed for use as a resonant tunnelling diode[26] or as a memory device[27].

This method cannot be used to measure single molecules and the fabrication process is harsh to the SAM. Even though the sample is held at liquid nitrogen temperatures for the evaporation, the SAM may still be damaged. Once the second layer of gold is deposited it is impossible to measure the orientation of the molecules or the state of the SAM.

The final approach for measuring the electronic properties of molecules is the nanowire method[28]. This method involves growing half of the wires into a track etch membrane, creating a SAM on top of that half and finally growing the second half of the wires on top of the SAM by electroless deposition. The wires are then freed from the membrane and placed in solution on top of a set of interdigitated electrodes with an alternating electric field applied between them, then the solution allowed to dry. The wires become attached across the electrodes and the whole surface is then covered with a dielectric allowing the properties of the SAM to be tested without shorting between the electrodes.

In this experiment the wire is simply lying on top of an electrode and covered with a dielectric. This raises questions as to how good the contacts are between the wire and the electrode and the question of a small leakage current through the dielectric. The group has gone some way to addressing this, as in the following paper, where the SAM are functionalised with OPE molecules, the wires have gold contacts evaporated over the ends but the whole device is still coated with a dielectric[29]. This method has not been used to measure single molecule properties although it has been used to measure multiple conducting molecular wires[29]. It was shown that stresses and strains on certain molecules and SAMs altered the electrical properties[19] and this is an issue with these nanowire devices. Also the state of the SAM inside the device cannot be measured.

The aim of this project is to measure the electronic properties of single molecules using a fabricated device. The project will share a lot in common with the method used by J. Mbindyo et. al. but with several differences. Wires will be grown in a similar way, but the way they will be contacted will differ. In this project the individual wires will be placed onto a substrate surface and photolithography will be used to contact them individually. This will place the wires under less stress than aligning them using an alternating electric field. Also the gold used to make the contact pads will be directly put down over the wire leading to a good contact. There will also be no need for a dielectric layer covering the device as there will only be one pair of contacts, which will have the wire between them, so there is little risk of shorting between the contacts.

The project will also aim to take the measurements further. After measuring, the SAM will be removed leaving a gapped wire which can then potentially have individual or very small numbers of molecules adsorbed across the gap and allow the properties to be measured. This should provide a good check on the data obtained by the SPM methods, the results having been gained by a simpler, more intuitive method with no need for complex post collection processing, giving much more direct results.

Molecular Conduction

The method of how the molecules studied in this project enhance conduction across a gap in a metal wire is shown in Figure 1, which is a diagram of the energy levels of a molecule between two pieces of metal. The Fermi energy is marked as the shaded area. As a voltage is applied, the Fermi level on one piece of metal increases in relation to the other which causes a breaking of symmetry of the system. If there was a metal in the gap this bias causes a charge to flow. If there was nothing in the gap, there are no energy levels for charge carriers to occupy so classically there can be no charge flowing.

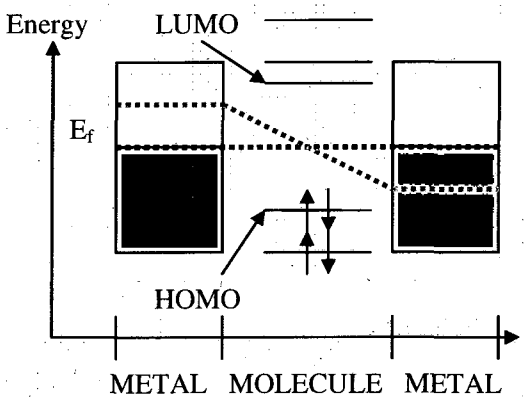

Figure 1. Diagram of metal – molecule – metal junction at zero applied voltage (black dashed line) and applied voltage (grey sloped dashed line) with negative potential on the left. A more complete diagram is shown in R. L McCreery[30].

In reality however, if the gap is small or the bias large a charge can flow without electrical breakdown via tunnelling. If there is nothing in the gap the tunnelling barrier is very large and consequently the chances of tunnelling occurring very small. If there is a molecule between the metals then the situation changes. In figure 1, LUMO is the lowest unoccupied molecular orbital and HOMO is the highest occupied molecular orbital. The LUMO cannot be below the Fermi level in the unbiased state otherwise it will become occupied hence the HOMO, however the LUMO can be just slightly above the Fermi level. If this is the case when a bias is applied the Fermi level of the negatively biased metal will rise above the LUMO allowing it to be occupied and conduction to occur in the conventional way. A more likely scenario, one which occurs with the molecules in this project is that the LUMO is significantly above the Fermi level of the metal. In this case, even a strong bias cannot raise the Fermi level high enough for conduction to occur before electrical breakdown occurs. In this instance the presence of a LUMO reduces the height of the tunnelling barrier increasing the chance of tunnelling occurring. This is referred to as an enhancement of the tunnelling current.

Fabrication Methods

The finished device consists of a pair of contact pads connected to a gapped nanowire. This is achieved by dropping the wires in solution onto a clean, oxide coated silicon substrate which is then coated with a positive photoresist and the pads and connecting features written using a Zeiss LSM510 direct write photo-lithography system. The pattern is developed and metal is evaporated over the whole surface. The remaining photoresist is dissolved removing any metal covering it leaving the completed device.

The methods described in this section are typical. The methods changed many times over the course of the project and these changes and why they were implemented are described in the Problems and Solutions section.

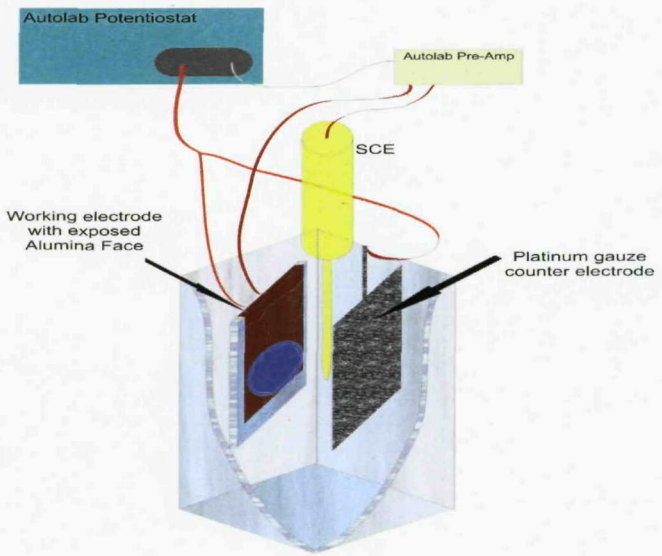

Figure 2. Shows the method used to deposit gold into alumina membrane

The wires are grown electrochemically into a 13mm diameter, 60μm thick Anopore alumina membrane with 200nm diameter pores. This is done by first coating one side of the membrane with gold in an Edwards 306A thermal evaporator. A 10nm chrome anchor layer is put down followed by around 250nm of gold. The gold side is then stuck to copper tape and mounted on a piece of glass slide. The whole face is then covered in clear nail varnish except the surface of the alumina membrane and the top section of copper tape which is used for electrical contact. This setup forms the working electrode of the electrochemical deposition setup using an Autolab PGSTAT30 potentiostat. The electrode is placed facing a platinum counter electrode and referenced using a saturated calomel electrode (SCE). Au wires were deposited from a fully bright cyanide-free commercial Au plating solution (Au concentration 10 g per L), (ECF60 and E3, Metalor, Cinderford, U.K.) with 5ml of brightener solution per litre of gold

plate added. This brightener solution contains arsenic which makes the grain size of the gold deposited smaller.

Before any deposition is performed cyclic voltammetery is run to determine the correct deposition potential, see figure 3. Of the three prominent peaks labelled 1, 2 and 3 it is peak 1 which shows the deposition potential. Peak 2 is the peak caused by stripping of gold from the surface and peak three is caused by oxidation at the surface. The voltage at which the minima of peak 1 occurs is recorded and amperometery run at that voltage. The amount of charge passed is used to control the length of the wires by the relation 1 C cm^{-2} μm^{-1}. This is determined from experience and states that for every square centimetre of alumina face exposed then one coulomb of charged passed will result in one micron of gold deposited down the pores.

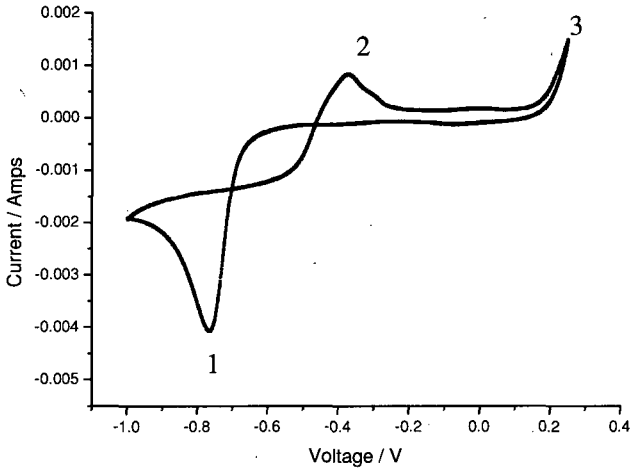

Figure 3. Cyclic Voltammogram of gold coated alumina membrane in commercial gold plating solution before deposition with peaks labelled 1, 2 and 3.

This gives some control over the length of the wires allowing a length to be picked that is long enough to contact but not so long that the wires fall apart at the gap due to structural stresses. In the instance shown in figure 4, five coulombs was chosen as the cut-off value. Given that our electrodes have an exposed face of approximately one square centimetre this would give the first half of these wires as 5 microns.

Once the first half of the wires has been grown a thiol is deposited down the holes to create a SAM. This has been done in a number of ways throughout the project. The following method is an example of a typical method with variations and alternates described later in the Problems and Solutions section.

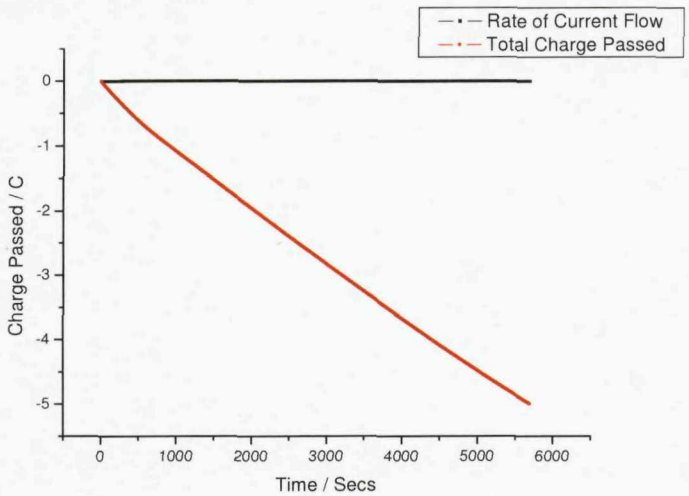

Figure 4. Amperometery plot showing amount of charge passed against time (red) and rate in Cs^{-1} (black).

Typically a 10 millimolar solution of thiol is made up using 1 – 16 mercaptohexadecanoic acid dissolved in methanol. The whole electrode is then placed in this solution and left for 18 to 24 hours. It is then transferred into a 10 mM copper perchlorate in methanol solution. This allows Cu^{2+} ions to adsorb to the double bond of the acetate group of the thiol and form a seed layer for the second half of the wire deposition. The electrode is then rinsed with ethanol and nail varnish reapplied to areas where necessary. A further cyclic voltammogram can be taken to determine the deposition potential with the SAM deposited but ordinarily this would not be done as there is a risk of stripping the adsorbed copper or the SAM. On the occasions it was performed it was found that the deposition peak had moved to a slightly more negative potential. The second half of the wire is usually grown at the same potential as the first half with the same cut-off value for the charge resulting in a wire with the SAM half way along.

To release the wires from the membrane the membrane is first freed from the electrode by dissolving away the nail varnish and glue on the copper tape by immersion in acetone. The free membrane is then stuck face down with nail varnish leaving the side with the gold evaporated onto it face up. This gold is then removed using potassium iodine commercial gold etching solution and gentle polishing with fine emery cloth. The membrane is then freed once more and stuck back down such that the original is returned to face up. This allows the wires, the ends of which will be exposed to be stuck and supported on a glass slide for the actual release. The membrane is dissolved away by placing into a 2 molar sodium hydroxide solution for twenty minutes. At this point there should be no more gas being evolved showing that the alumina has completely dissolved. The supported wires are then put into a vial of isopropanol alcohol (IPA) and sonicated to be released. They are left to settle for 24 hours and the IPA is replaced to rinse any remaining sodium hydroxide and small particulates out of the solution. This rinsing is repeated three times leaving clean wires suspended in IPA.

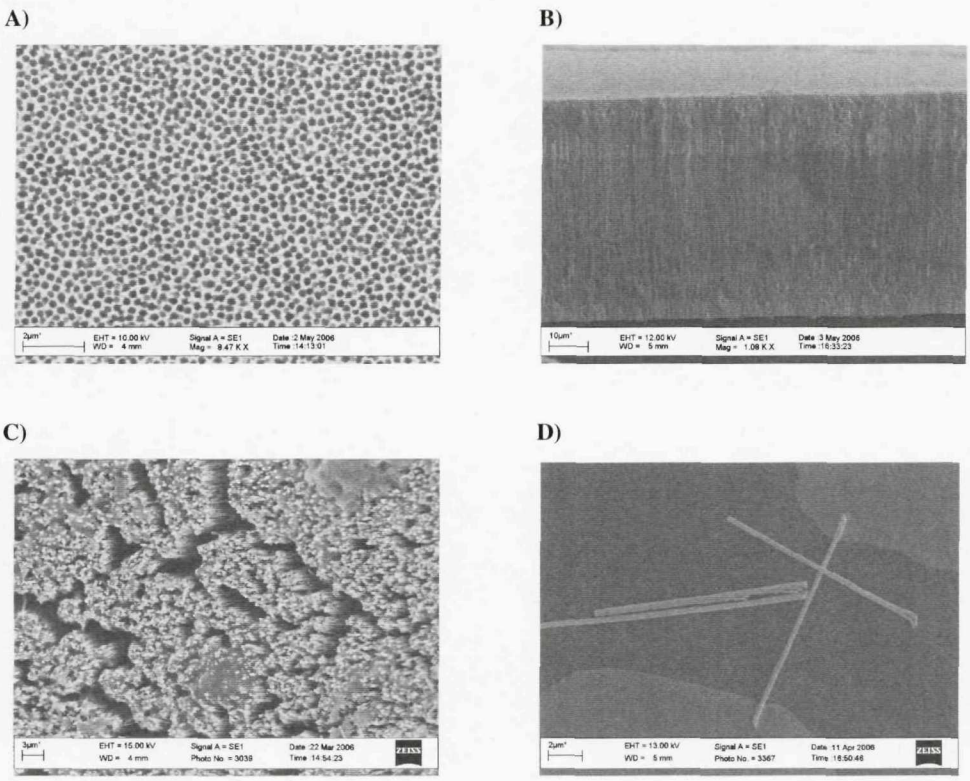

Figure 5. SEM images showing wires at different stages of growth. **A)** The surface of the membrane the wires are grown into. **B)** A cross section of the membrane after the wires have been grown. The arrows show the position on the back surface and the ends of the wires. **C)** A forest of wires after the alumina membrane has been dissolved. **D)** Some released wires on an oxide coated silicon substrate.

Scanning Electron Microscopy was performed on individual wires to image the gap in the wire as shown in Figure 6. Whilst this was attempted on single SAM gaps, they proved too small to be imaged so wires with gaps formed with multiple SAMs were used. The wires shown in Figure 6 were produced with six self assembled monolayers. A number of the wires in this figure show clear gaps within this field of view and most of the wires show gaps at some point along their length.

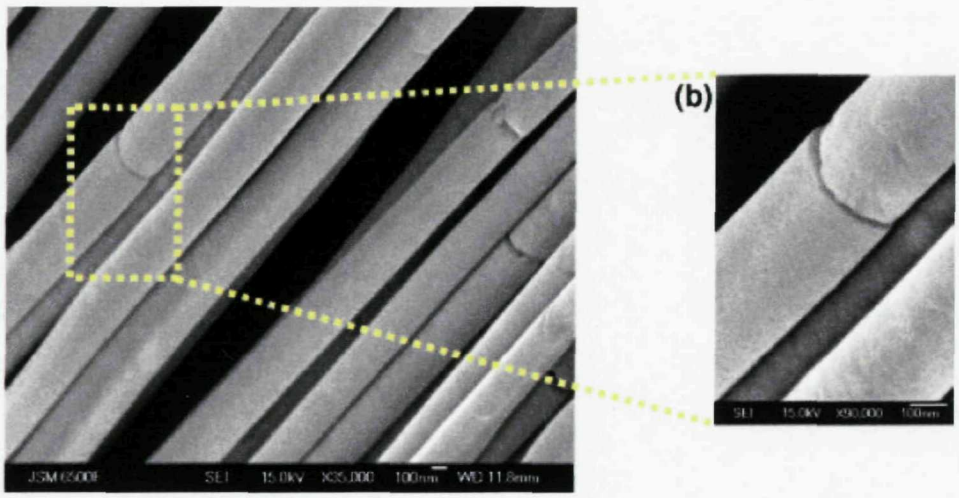

Figure 6. SEM image of gold nanowires with a six layer 16-mercaptohexadecanoic acid self assembled monolayer. Courtesy of C. Gardiner, M. Ghanem et al[1].

The first concern when making a device by photolithography is a clean substrate. To get the oxide coated silicon substrates as clean as is necessary they are sonicated at full power in a 20kHz bench-top ultrasonicator for 60mins in individual vials of Sigma Aldrich ReagentPlus grade 2-propanol. They are then dried with compressed air such that the solvent leaves no residue.

Five to ten microlitres, depending on the concentration, of wire solution is then dropped onto the surface and the suspending IPA left to evaporate leaving the wires spread randomly about the surface. A layer of S1813 photoresist is spun over and baked at 116C for 1 minute. The sample is then taken to a Zeiss LSM510 laser scanning microscope to write the pattern into the resist. This is done in two stages. Using the optical microscope a suitable wire is found which looks approximately the correct length, is straight and in a clean area on the sample. This wire is then imaged and measured using a HeNe laser at 543nm in the laser scanning microscopy (LSM) mode. The large contact pads are then written around the wire using the 458nm line of a 40mW, continuous wave, air cooled argon ion laser, a 10x lens, a laser power of typically 75% of its maximum and transmission of typically 80%. Once the contact pads are written the lines connecting the large scale pads and the small scale wires can be drawn. For this the 40x lens is used. The centre of the device including the wire is scanned using the LSM mode and the pattern for the connecting lines put in place. They are then bleached at much lower power, typically 30%, and lower transmission, normally 50%. This allows smaller features to be written by bleaching less of the resist around the area the laser strikes the surface.

After the pattern is written the sample is soaked for two and a half minutes in chlorobenzene which generates an overhang meaning there is a gap between the gold that is to remain and that which is to be rinsed away giving better results at the lift off stage. The resist is developed using Shipley MF319 developer solution. Developing is performed on the spin coater allowing precise control over the amount of time the developing solution is applied. The spin cycle is repeated until the pattern is completely developed.

The next step is to place the developed devices in an Edwards 306A Thermal Evaporator where a 5nm chrome anchor layer is put down by evaporation from a tungsten basket at 6 x 10^{-6} mbar followed by a 25nm layer of gold from a molybdenum boat at the same pressure. Any thicker than 25nm results in poor lift-off because the areas to remain become joined to those that are to be removed by a gold layer.

The final stage is to soak the devices in acetone which will dissolve the remaining resist taking any gold layered on top with it. It was found that best results came from leaving the devices to soak for approximately 10 minutes until some peeling of the gold was observed. Then acetone is squirted gently from a pipette onto the centre of the actual device such that the gold peels away from the pattern outwards. This resulted in many fewer devices having strands of gold left behind connecting between the pads.

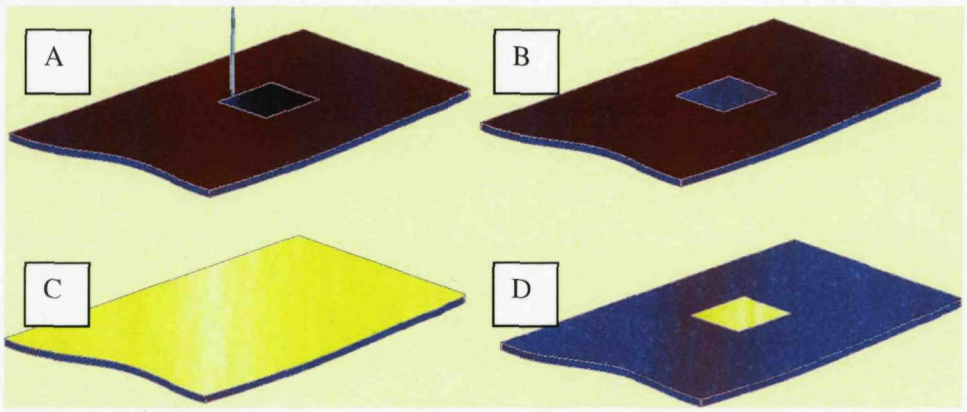

Figure 7. A. A laser is used to write a pattern into the resist coated onto silicon oxide substrate. **B.** The pattern is developed. **C.** Gold is coated over the whole surface by thermal evaporation. **D.** Acetone dissolves the remaining resist, which takes away the overlying gold leaving the pattern.

Problems and Solutions

A significant amount of time was spent on each stage of the fabrication process in an attempt to increase the overall numbers of devices that were completed and tested. The single biggest problem throughout the project was with wires that measured as ohmic. Although the reason for these ohmic wires is not certain it seems likely that it is caused by gold fibrils forming at SAM defect site. The application of a copper layer immediately after the SAM was put down was to make the event of a gold contact running between both halves of the wires a lot less likely as the gold for the second half would seed at the sites where copper was present and the relatively large copper atoms would go some way to blocking any holes in the SAM. The first change that was made was from using a methanol based copper-perchlorate solution to an aqueous copper sulphate solution. This allowed the following reduction to be performed in the same aqueous solution of 0.1M boric acid and was done by running a cyclic voltammetery measurement form 0.5V to -0.8V but not back, ensuring a pass of the reduction potential but not allowing the stripping potential to be passed on the return. This made the copper 2+ ions deposited from solution into atomic copper. A further benefit was that once the SAM is deposited it does not come into contact with methanol. The SAM is not soluble in aqueous solutions so holding it in the copper containing solution should not affect it.

The way the gold was deposited was also varied over the course of the project by the use of arsenic brightening solution. This solution lowers the grain size of the gold which may create a more planar interface at the SAM site. However both the arsenic and copper additions, as well as not being strictly necessary, are bad for the final measurements as the arsenic is effectively an impurity in the gold and a copper layer means the junction is not symmetrical. The process was attempted without either copper or arsenic, with one not the other and with both, however no one configuration resulted in significant increase in yield.

The next step was to attempt to increase the integrity of the SAM. The gap size in the wire is determined by the SAM so that is not open to change. The first stage of the SAM deposition continued as usual with a 24 hour soak in a mercaptohexadecanoic acid to form a SAM with a length of 16 carbon atoms in the chain. This was followed by soaking in mercaptoundecanoic acid which forms a shorter SAM with 11 carbon atoms in the chain. It follows that the only place to which the shorter SAM would be attracted would be any exposed gold by the same mechanism that the longer chain is attracted. This would plug any gaps in the SAM and allow copper to bond with its top surface creating seed sites. The same idea was also attempted with 1-6 haxanedithiol molecules which form a much shorter 6 carbon chain SAM. These shorter molecules would travel down any holes more easily but do not allow copper to seed to their top surface due to the lack of the acetate group. It was hoped that these methods would create a denser SAM with few or no holes.

A further reason wires could be ohmic is if during the release procedure the gold etch solution etched through the back layer of gold and then down the pores through the first half of the wires leaving just the solid gold second half. The rate at which the etch solution etched was carefully checked and discounted as it took a significant amount of time, the order of minutes, to remove the 250nm of gold covering the reverse of the membrane. It would have taken far longer to etch the 4 – 6 microns of gold that make up half of a wire compounded by the fact that the etching would have occurred down

the pores of the membrane limiting the rate of transport of gold away from the surface meaning the etching would have taken longer still. A far more likely source of problem during the release process was during the sonication stage where the free wires were released from the surface. This was a stage with conflicting ideals. Ideally the wires would be sonicated for as short a time as possible, but also at as low a power as possible. The problem was that they needed quite a powerful sonication to get any release at all. So a balance was struck sometimes sonicating at lower powers for longer times and others at high powers for a very short time. Ultimately little difference was recorded but SEM images of released wires perhaps provided the answers as to why so many devices turned out to be ohmic.

In a particular set of SEM measurements taken late on in the project on unreleased wires still in the membrane, the wire length was measured at twice the expected length. This was confirmed by growing the next set of wires to be half the ten microns they would normally be. They measured as ten microns when unreleased in the membrane. Since not all devices measured as ohmic with some giving correct breakdown responses clearly not all were snapping at the gap. This leaves two possibilities as to what is happening.

The first is that all wires with no SAMs or defective SAMs with gold contacts formed through them grow to twice the expected length, due to the increased efficiency of gold deposition. Wires with good SAMs grow to the correct length. There are only a few wires with good SAMs which are hidden in the SEM images by all the longer wires. The stresses on the long wires are large causing them to snap into two parts. This would explain the spread of wire lengths seen and large proportion of ohmic wires. The second idea is that all the wires have good SAMs but they all grow to twice the expected length with most of them snapping in the middle on release forming a lot of ohmic wires. Some snap at a point other than the middle leaving the SAM in tact and giving good measurements.

Although both these ideas are plausible there is little that can be done to test them or rectify the problem. They cannot be tested as there is no simple method for seeing where the gap in the wire is. There is not a lot that can be done to remedy the problem as the wires still need to be released. Furthermore if either of the theories is correct they do not help us pick a wire to contact as a gapped wire and an ohmic wire look identical.

As changes were being made to the ways wires were grown, there were also significant changes made to the design and method of the device and its fabrication. Devices would fail in one of four main areas. They could fail at the development or lift off stages of fabrication or fail during testing due to poor contacts that were either badly made or broken during the test.

At one point in the project the number of devices that failed to develop correctly increased dramatically although there was no change to the procedure. This was identified as a chemical problem with the resist which had gone bad. A simple change such that a small amount of resist was taken from the main stock each time rather than keeping a larger amount separately fixed this problem. The development itself was performed on a spin coater rather than simply dipping the sample into developer as the spinner allowed greater control. By the end of the project the development process was reasonably refined but there would still be a small fraction of devices lost here. This is down to the fact that the patterns used were fabricated in two parts, the large contact pads and the small contacting lines which used different lens and required different laser powers and percentage transmissions and different bleach times. This means that the resist for each part would not be bleached exactly the same

amount so one section would develop faster that the other. If the larger pads developed slightly quicker it was not normally a problem but if the smaller features developed faster it was an issue as the small features would have joined together before the larger ones were well developed. Since the rate at which the resist developed was strongly dependent on its thickness and any particulates under it, it was not always the case that the large features were developed by the time the smaller ones were joined.

Devices failing during lift-off was a significant problem with as many as half of any batch being lost at this stage. The first change was the technique of how the lift off was performed. At the start of the project the batch of devices would be left in an acetone bath until the gold was seen to crinkle. Then acetone was gently squirted from a pipette from the side to peel the gold away. This technique coupled with the original design of the device meant that gold would be shielded from the acetone flow and remain in place around the centre of the pattern often causing contacts between pads. Sometimes further soaking would remove this but often not. The technique was changed such that the acetone was squirted directly down over the centre of the device so there was a flow outwards in all directions over the device resulting in better lift off. The design of the device still had very small features and channels that did not lend themselves to easy lift-off so the design was changed.

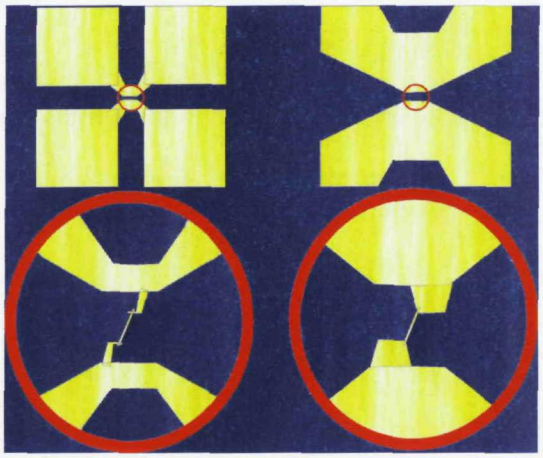

Figure 8. Left hand device shows original design, right hand shows new design. Bottom figures are enlargements of centre area

The modifications that were made are shown in Figure 8. There were two main changes, the first being the contacts to the wires themselves, the second being the gaps between the pads. The contacts were changed so they were thicker with no unnecessarily small features which were prone to either developing with gaps in and over development. There are also no small cave like areas in the design which encouraged gold to remain stuck to the surface (See figure 9).

In the second design there are only two pads as required. The original design was made with four point measurements in mind but the extra pads proved unnecessary in this project as only two point measurements were ever made. The problem with lift off would come when a bit of gold remained contacting the pads in parallel with the wire. This is much less likely in the second design as

the gap between the pads is much larger and the gradient towards smaller features more gentle resulting in much more successful lift off.

The final main point of failure was during testing. This could either be discovering during a test that the device gave no response meaning that the contacts were not good or that they had very small fractures not visible with the microscope. This was partly resolved by the change of design as the contact lines no longer had very small features connecting to the wire but there would still be a number of devices in every batch that would give no response.

A more interesting method of failure during testing was at a late stage after the gaps had had the SAMs cleaned out and attempts were made to introduce molecular wires. Devices that previously gave good responses at all stages of testing were suddenly giving no response at all. It was found that if the toluene the molecular wires were suspended in were allowed to evaporate there was a good chance it would lift the contacts away from the wires due to toluene becoming trapped in the gap under the contact around the edge of the wire. The only solution here was to perform all of these experiments under toluene and leave the device permanently under toluene for storage, never allowing it to dry.

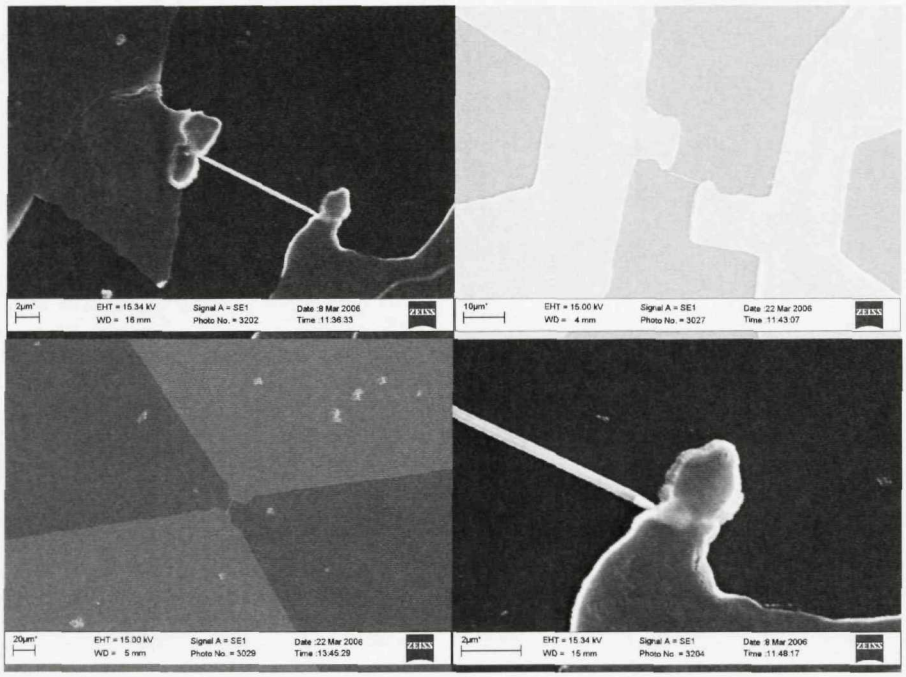

Figure 9. Four SEM images of devices. **A**) Shows how gold would often not lift off around the contacts of the old style device. **B**) Shows how the old design should look. **C**) Shows the new style design. **D**) Shows how toluene split the contact between the wire and the contact.

Experimental Section

Once the devices are complete they are measured using a two point measurement with an Agilent 4155B Parameter Analyser.

It should be noted that all measurements in this section are performed using a 2 probe approach rather than the 4 probe approach. Whilst in principle it is true that a 4 probe measurement would provide more accurate results by allowing a determination of contact resistance in our case however this was deemed not necessary. The reason for this is that the resistance of an ohmic wire, as shown in figure 10 is measured as around 30Ω. This value places an upper limit on the associated contact resistances in the system of around 30Ω. A similarly fitted gapped wire with the SAM present, with a gap or with molecular wires adsorbed gives a measured resistance of approximately 10^{12}Ω. In any of these cases, clearly the contact resistance is negligible. As this project is not concerned with the properties of ohmic wires the decision was taken to not include four point measurements as there is considerable extra difficulty in the fabrication of a device with contacts for four probes.

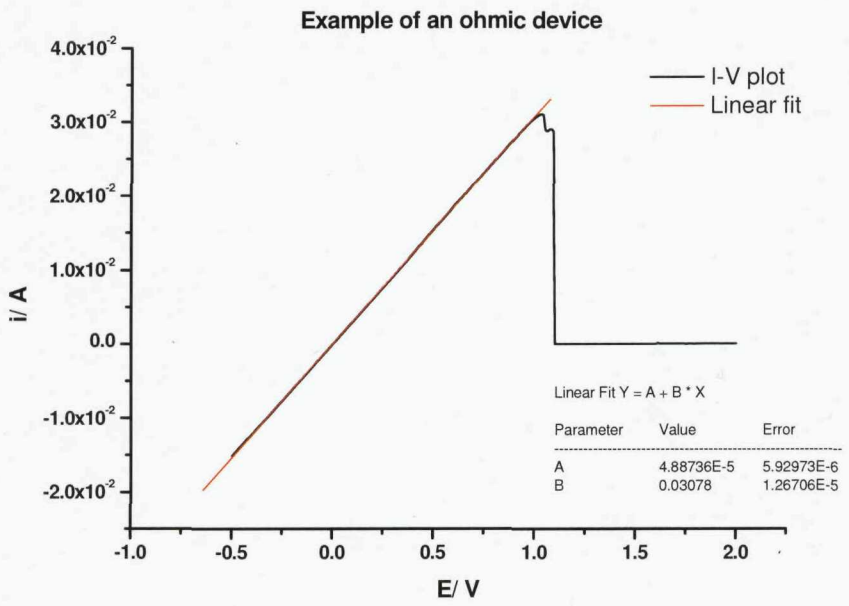

Figure 10. Example of an ohmic device. The wire in the device conducts with ohmic characteristics until it fails due to too high a current load. The ohmic section is fitted, where the inverse of the gradient is the resistance of the wire. R = 32.5Ω.

A standard measurement scans the potential difference from a set low value, typically -0.5V to a set high value, normally around 2.0V at a constant rate, typically in 10mV steps. All measurements are performed using the long integration time setting.

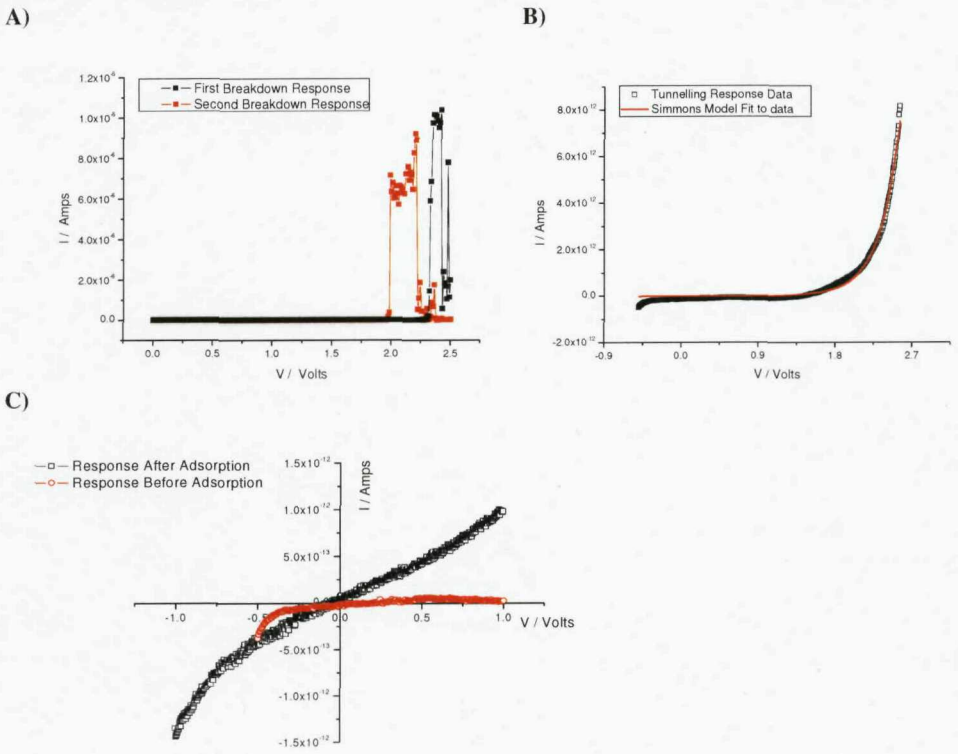

Figure 11. A) A representative response of a wire with a SAM in the gap. The black line is the first measurement and the red line is the result of an identical measurement immediately afterwards. **B)** A typical tunnelling type response after the SAM has been removed. Fit shows gap size of 20.5 ± 0.06 nm and a barrier height of 2.44 ± 0.01 eV **C)** A tunnelling response (red) and the enhanced response if small molecules are adsorbed across the gap (black). Data in this figure is from set 3 of the results presented below.

A first measurement is performed after fabrication when the wires have been contacted and the gaps should be filled with the SAM. If this is the case then a breakdown response is observed (see figure 11). This is because as the voltage is increased then at some point the electric field is sufficient to cause electrical breakdown and whilst there is not enough information to be certain of the exact mechanism, it is certain that this breakdown permanently alters the contacts or the SAM. This breakdown response is measured as the peaks shown in figure 11A. If this measurement is then repeated the peaks will be at a lower voltage due to the quality of the SAM being degraded from the first electrical breakdown or because the gap has become smaller due to gold electro-migrating across the gap. If the measurement is repeated enough times the response will become an ohmic one as gold electro-migrates through the lower quality SAM due to the potential difference applied. Indeed some people use electro-migration techniques to create small gaps in gold wires (see Introduction) but here it

is an unwelcome side effect which is limited by stopping the measurement as soon as breakdown is observed and not repeating it in most cases.

Once a breakdown response has been observed across a SAM in a device, that device is placed in a furnace and heated within the range 200°C to 260°C in air for one hour to remove the SAM. Many variations on this were attempted throughout the project changing both the temperature and the time; however the values given above yielded the best results. Extending the time for longer than an hour didn't produced any noticeable difference. A lower temperature resulted in the SAM not being completely removed from the gap and a higher temperature increased the likelihood that a device would measure with an ohmic response as the gold becomes softer and more mobile at higher temperatures. This becomes a problem as the aspect ratio of our gaps is high, with the wires being 100nm in diameter and the gap being 20nm wide. Aside from heating, several other methods of removing the SAM from the gap were attempted. These include piranha etch, where the device is placed in a solution containing a mixture of sulphuric acid and hydrogen peroxide to chemically break down the SAM, plasma etch, where an oxygen or argon plasma is used to break down the SAM and ozone treatment where a UV lamp is used to generate ozone within the SAM which can then break up the SAM. None of these methods gave better electrical results and the device failure rate was not improved.

After heating the wires are again electrically tested but starting with a small range in potential difference which is increased in 0.5V increments until a tunnelling response is observed. The tunnelling response is expected as the electrons can tunnel through the air but there is no breakdown response swamping the signal (See figure 11). Once a tunnelling response is observed it is consistent and repeatable. Electro-migration of the gold does not happen noticeably as the potentials required to observe the tunnelling response are lower and the currents passed are much lower. Any changing of the gap size would be apparent as an increase in the tunnelling response as it is very sensitive to the gap size.

This strong dependence of gap size allows us to use the tunnelling characteristics observed to accurately predict the size of the gap using the Simmons tunnelling model[31] according to the equation below.

$$J = \left(\frac{e}{2\pi hs^2}\right)\left\{\left(\varphi_0 - \frac{eV}{2}\right)\exp\left[-\frac{4\pi s}{h}(2m)^{1/2}\left(\varphi_0 - \frac{eV}{2}\right)^{1/2}\right] - \left(\varphi_0 + \frac{eV}{2}\right)\exp\left[-\frac{4\pi s}{h}(2m)^{1/2}\left(\varphi_0 + \frac{eV}{2}\right)^{1/2}\right]\right\}$$

This equation includes parameters for the gap size s, the potential applied V and the tunnelling barrier height, φ_0. Symbols e and m are the charge and mass of the electron and h is planks constant. Since the voltage applied is known, a curve can be fitted to data to give the barrier height and gap size. Qualitative observation suggests that the gap size given is accurate, as molecules can no longer be measured to have adsorbed across a gap when the size is predicted as too large and are in good agreement with the thickness of the SAMs used to make the gap[32].

Once devices have been identified with wires having suitable gap sizes molecules can be adsorbed across the gap. The choice of molecule depends on the size of the gap but is typically oligo-phenylene-ethynylene (OPE – see figure 12) for smaller gaps and a five benzene ring variant of the

same molecule for larger gaps. The molecules are dissolved in toluene and applied to the device to allow the molecules, the ends of which are attracted to the gold, to adsorb across the gap. A repeat of the measurement should reveal an enhancement in tunnelling current due to the increased conductance of the gap with molecules present.

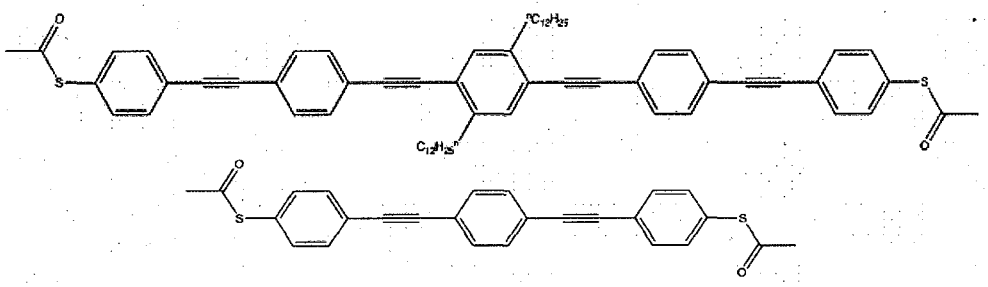

Figure 12. Top molecule is 1,4-bis(2-(4-(2-(4-thioacetylphenyl)ethynyl)phenyl)ethynyl)-2,5-didodecylbenzene. It is referred to as the 5-ring wire in this project. The bottom molecule is 2,5-di(phenylethynyl 1-4' – thioacetatyl)benzene more normally known as oligo(phenylene ethynylene) or OPE for short. It is referred to as 3-ring wire in this project.

Results

Below is a table showing the number of devices that made it through to various stages of the testing process. It shows the total amount of devices that were started and the amount that successfully completed the fabrication process in the first two columns. The other three columns are testing results, the third showing how many devices that showed a response that was not ohmic, the fourth column showing the amount of those that gave a tunnelling current after heating and the final column showing how many had an observed difference in the response after molecular wire adsorption.

	Devices Started	Devices Completed	Non Ohmic Responses	Tunnelling Responses	Successful Adsorption
Number	422	295	52	12	5

The 422 devices were typically made in a batch of ten. A single batch would take a full working day to pattern, coat with resist and prepare for the evaporator. It would then take a further day to evaporate gold onto the surface then chemically remove the excess gold leaving the final device. As the table shows there were two major areas of loss. For a full breakdown of devices started and where they failed see appendix 1, (Device table). There were 127 devices lost in the fabrication process over the entire project which equates to 30% of all devices started. Improvements were made over the course of the project. In the first 12 batches, each containing ten devices, there was a 38% loss rate at the fabrication stage compared to a 26% loss rate in the final twelve. This figure is still high and could be improved significantly, perhaps with the use of a dual layer resist.

The highest area of loss was the completed devices that either gave no response, an ohmic response or a spike response which would then give no response. A total of 243 (42%) devices were lost in this way, which breaks down as 135 (32%) showing ohmic responses. 69 devices in total (16%) showed no response at all when tested despite appearing complete and connected when viewed optically. A total of 20 devices (5%) spiked and failed during the test. This failure method can be attributed to small gold filaments migrating through gaps in the SAM due to electro-migration.

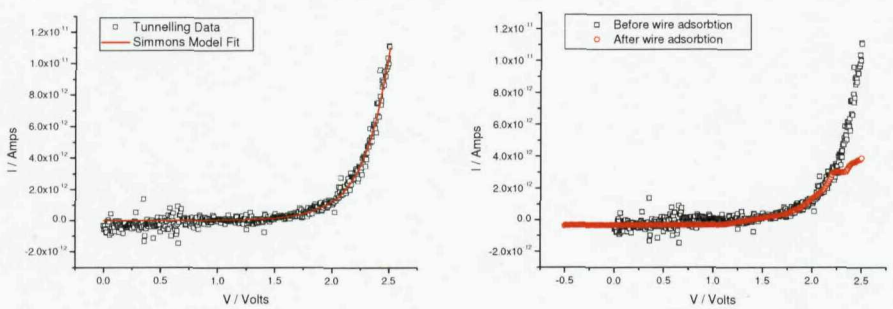

Figure 13. Graph A is of the tunnelling response predicting gap size of 20.0 ± 0.14 Å and a tunnelling barrier height of 2.35 ± 0.01 eV. Graph B is the same wire with results for before and after molecular wire adsorption.

The first experiment shows an example of a tunnelling response which has had the Simmons tunnelling model applied to it giving a gap size of 20.64Å. It was than placed in a bath of 3-ring molecular wires and re-tested. Figure 13B shows the result, the black line being the original tunnelling response the red line being the response after the experiment. There is no change showing that no wires adsorbed across the gap. This can be understood by considering the angle at which the molecular wires will adhere to the end of the gold wire. The 3-ring molecular wire is 20.67 Å long but the sulphur bonds to the gold with a bond angle of 30 degrees, so the maximum gap a 20.67Å molecular wire could span is:

$$20.67 \text{ cosine } 30 = 17.90 \text{ Å}$$

This means that any single wire could not bond to both sides of the gap so no response was seen. A five ring adsorption experiment would have been more appropriate in this case, the five ring wire being 34.58 Å in length allowing it to span 29.95Å.

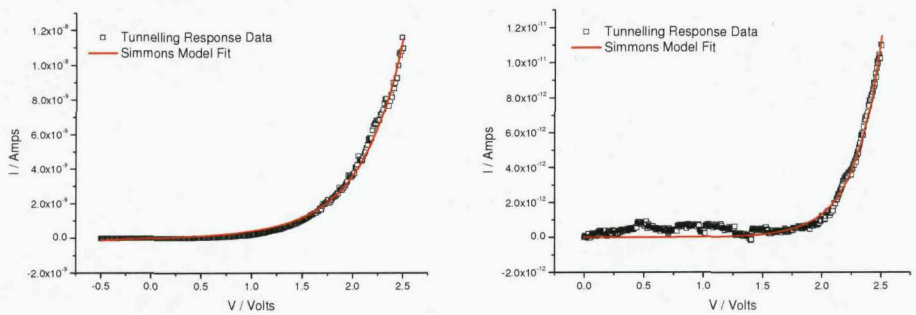

Figure 14. A) The tunnelling response of a device immediately after heating giving a gap size of 13.1 ± 0.05 Å and a tunnelling barrier height of 2.75 ± 0.01 eV. **B)** The response after 3 ring wire adsorption giving a gap size of 20.5 ± 0.15 Å and a tunnelling barrier height of 2.37 ± 0.02 eV.

The second experiment shows the tunnelling response and predicted gap sizes before and after a 3 ring adsorption test and the measured resistance of the wires. This is an odd case where the conductance of the device actually decreased after the adsorption experiment suggesting the molecules have not bonded properly with the gold and rather just clogged the gap. This could be caused by the gap not being thoroughly cleaned during the heating phase leading to an incorrect prediction of gap size or not allowing molecules to properly bind during adsorption.

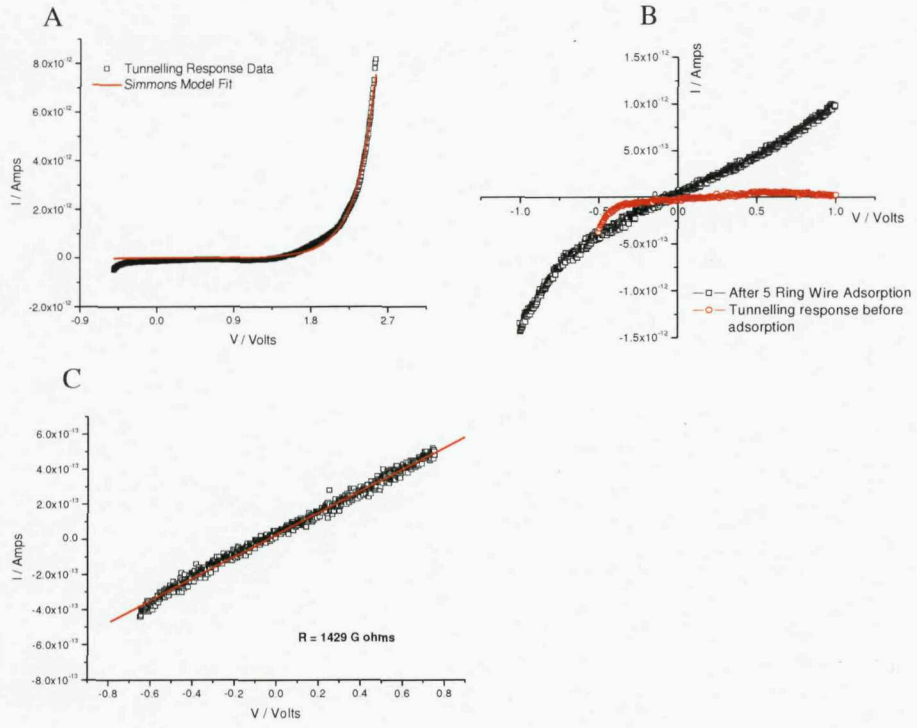

Figure 15. A) The tunnelling response after heating giving a gap size of 20.5 ± 0.08 Å and a tunnelling barrier height of 2.44 ± 0.01 eV. **B)** The response before and after molecular wire adsorption. **C)** The linear fit used to calculate the resistance of the device with molecular wires adsorbed across the gap.

The third experiment shows the tunnelling response and a Simmons fit giving a gap size of 20.50Å therefore the device was put into a solution containing a 5 ring wire. Figure 15B shows that there was a noticeable enhancement in the current (the red line is the original tunnelling response and the black line is the enhanced response after adsorption). For positive applied bias, where the initial charging current associated with the start of the run observed at -0.5V on the red curve has decayed, the current is increased by a factor of 8.5. That is to say that when the associated molecules bridge the gap over 88% of the current flow is through the molecules and not through other possible parallel conduction paths i.e. the substrate. This experiment also allowed a simple linear fit to be performed to determine the resistance. Whilst over an extended range of potential difference the molecule bridged gaps are non-ohmic in behaviour they do show a potential range over which the current-voltage relationship is linear. It is not clear why this linear region exists and what controls its potential range. However we, like others in the field, have fitted this linear portion of the current-voltage relationship to obtain a resistance, 1492GΩ, which can be associated with the conduction through the molecules to enable comparison with other reported results. Whilst the resistances obtained from these fits make comparison easy it should be born in mind they only characterise a limited part of the current-voltage characteristic and they do not imply the molecules are ohmic.

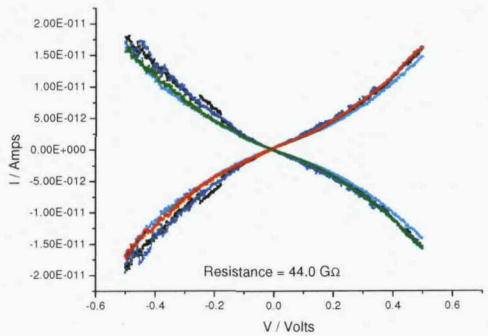

Figure 16. Measurements of a device that has been left in a three ring wire solution for an extended period of time.

The fourth experiment shows the results of leaving the device in the molecular wires for different amounts of time. The device was placed in and contacted. A scan was run straight away, then again after fifteen minutes, again at thirty minutes and finally after a weekend of soaking in the solution. There is a response showing a linear region around zero potential as is expected after the addition of the molecules. However the response does not increase with time. This suggests that any molecules that bond to the ends of the gold wire do so quickly compared to the time of the first measurement, and that the ends of the wire get saturated with molecules or the molecules get depleted from the solution such that there are no more to adsorb. Despite seeing no increase a good resistance measurement was made and gave a value of 44.0GΩ.

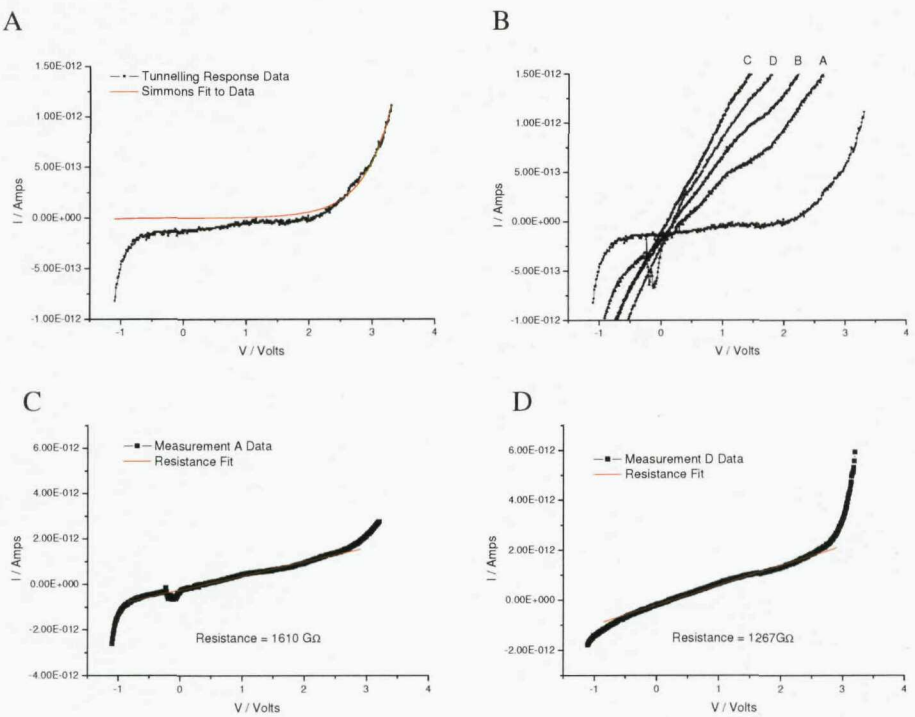

E

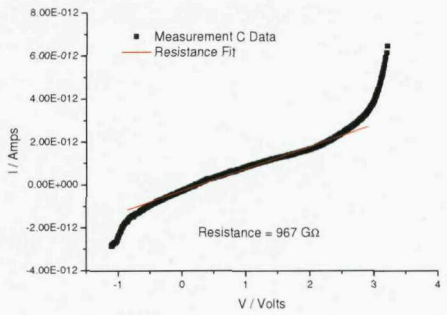

Figure 17. A) The tunnelling response of a device after heating giving a gap size of 16.0 ± 0.49 Å and a tunnelling barrier height of 4.14 ± 0.18 eV. **B)** Response before and after a 3 ring wire adsorption experiment where the device had been left in the molecular wire solution of different amounts of time. **C) – E)** Resistances measured after different times in the molecular wire solution.

The fifth plot is again of I-V characteristics taken at different times during an experiment to attempt to measure adsorption over time. An I-V measurement was performed immediately before the device was put into a solution containing the molecular wires. Another I-V measurement was performed immediately after and then at intervals of 1000 seconds during which the rate of current flow was recorded. The results show no noticeable rise in current passed with time, although the I-V set presented does show some change in resistance after each time measurement. However it still suggests that most of the change happens rapidly at the start. Also it should be noted that the resistance measurements recorded for the I-V curves on this experiment are very high, the first curve after the adsorption revealed a value of 1610GΩ and the final curve of the set showing a resistance of 1267GΩ. This is a substantial drop of 343GΩ but the validity of this result is questionable due to the extremely high resistances measured for a 3 ring wire contrary to other results that have be seen previously in this project and those in the published literature. Another dubious aspect of this experiment is that the lowest resistance of 967GΩ was recorded for the penultimate graph of the set not the final one which had been in the solution the longest as would be expected. Also this result is significantly different from the final value by 300GΩ suggesting that the real error in the measured resistance could be of the order of 300GΩ. This is around the value the measured resistance changes over the course of the experiment so any conclusions drawn about how the resistance changes over time would be debateable.

The small numbers of results makes drawing conclusions difficult. Of the three successful three ring wire experiments, resistances of 76.92GΩ, 44.0GΩ and 1610GΩ have been measured. Whilst there are not enough results to be certain it appears as if the 1610GΩ result is an outlier. Although the results are limited they do compare favourably to values measured by the conducting AFM method which were 51 ± 18GΩ[19] and significantly higher than the values measured by STM which were 1.7 ± 0.4GΩ and 1.9 ± 0.5GΩ in film form[20].

The result obtained for the five ring wire is difficult to compare to any results in the literature as the specific five ring wire used does not appear and any changes to the molecular structure can

significantly alter the properties of the wire. This is demonstrated by figure 1, in a paper by James M Tour[26] which shows a current – voltage plot for a molecule with five benzene rings. This plot can be used to infer a resistance for the molecule of $0.266G\Omega$ which is a factor of 5000 smaller than that measured here. This is not a comment on the accuracy of either set of results, just to say comparing different molecules is not sensible. As there is only one result obtained for the five ring wire it is not possible to say anything about the accuracy beyond that it is significantly higher than that of a three ring wire as would be expected. It is not even possible to estimate how much higher than the three ring wire, the five ring wire should be as the five ring wire has alkyl groups attached to the middle benzene ring which the three ring wire does not.

Summary and Conclusions

This project started by reviewing different methods of contacting molecular wires and measuring the electronic properties. All of the methods have advantages and associated problems, not least that the most reliable techniques for contacting and measuring molecular wires could never be used in working devices and of the methods that could conceivably be incorporated into a working device, it is impossible to know the precise conditions of the molecular wires and to measure single wires. The goal of this project was to attempt address these issues and fabricate by photolithography a device with the potential to be included in a real working system and with the ability to measure the electronic properties – hence contact – single molecules.

The designed method for achieving this was to grow gold wires with nanometer diameters and micron lengths, with a self assembled monolayer gap as close as possible to the middle of the wire. The micron scale length allows the wire to be contacted by photolithography. The SAM in the centre can then be volatilized away simply be heating leaving a contactable device with a nanometer sized gap. This was then to be put into a solution containing molecules with functionalised end groups which would bind across the gap allowing measurement of the resistance.

The project demonstrated that this method can work and can be used to contact and measure the electronic properties of small numbers of molecules. In the results that have been seen the method suffers from a similar problem of many of the other techniques in that the exact numbers of molecules in the gap cannot be known. However the method has the potential to know this simply by reducing the concentration of the conducting wire solution until it is so low that the jumps in current due to individual wires can be seen. This would be an ambitious experiment but there is no reason in the design of the device that would make it impossible.

The results that were gained although very low in number compare well to the results obtained by A. M. Rawlett's conducting atomic force microscopy experiment[20]. Both of these sets of results are appreciably higher that those obtained by A. S. Blum's experiments with a scanning tunnelling microscope[19]. This is strange as the STM method has the most support in the literature and is the most convincing in terms of actually contacting a single molecule. If this is the case and cAFM and the method used in this project are contacting more molecules then the resistances measured should be lower than those measured by STM.

Ultimately more measurements from the method used in this project would have been very useful in the field of molecular electronics. It is not impossible to get many more measurements from the technique but it would be very time consuming. This is the major problem faced by anyone continuing with this type of device. To make it a viable method many more devices need to get completely through the fabrication stage. Ideally to achieve this there would be some method of contacting wires that did not involve searching for and individually contacting single wires as this is where most of the effort goes. If such a technique could allow for contacting 100 nanowires per week, then meaningful results would be forthcoming on a monthly timescale even with the nanowire gap quality statistics remaining the same. In reality the method of growing the nanowires would have to be refined in parallel with the contacting procedure. There are two obvious next steps to be attempted in the nanowire growth procedure both present in J.K.N. Mbindyo's paper on nanowire growth[27]. The first

is to cap the top of the SAM by an electroless seed method before electrochemically depositing the SAM. This would mean the gold put down on top of the SAM initially would not be attracted by a potential difference down any defects and could increase the quality of the resulting SAM. The second procedural change that is likely to have an impact could be the use of polycarbonate track etched membranes which readily dissolve in dichloromethane. This could help in removing the sonication step in the method, of which as mentioned in the Problems and Solutions section, there is at least some evidence to suggest was causing wires to break apart.

In summary this project has shown it is possible to fabricate devices using photolithographic and electrochemical methods that can contact molecular wires. It has succeeded in its stated aim of characterizing the gaps in nanowires and measuring electronic properties of molecules albeit in very small numbers, though this was through no flaw in the design of the device but rather in the practical aspects of getting every stage of the fabrication process to be successful. Of the few devices where this was the case, experimental results were forthcoming in all but one of them. The project was not successful in contacting a single molecule, but there is no reason why a device with this design could never contact a single molecule. With more working devices to use, observations of steps of current increase should be achievable given the unique way the method can measure the electronic characteristics of the gap as the molecular wires are adsorbed across.

Appendices

Appendix 1. Device Table. Non-ohmic column [Number (Ohmic / No response / Spike]

Batch Date	Started	Completed	Non-ohmic	Tunnelling	Adsorption
23/11/05	5	5	1 (2/2/0)	0	
25/11/05	10	8	4 (2/0/2)	0	
29/11/05	10	7	3 (1/3/0)	0	
01/12/05	10	5	1 (0/4/0)	0	
06/12/05	10	6	5 (1/0/0)	1	0
08/12/05	10	10	2 (5/2/1)	0	
12/12/05	12	0			
15/12/05	12	6	0 (4/2/0)		
20/12/05	10	7	0 (5/0/2)		
05/01/06	10	6	0 (3/3/0)		
06/01/06	10	10	2 (5/3/1)	2	1
09/01/06	10	7	0 (5/1/1)		
12/01/06	10	8	0 (5/0/0)		
19/01/06	10	10	0 (5/1/0)		
01/02/06	10	7	1 (3/3/0)	0	
02/02/06	10	9	3 (4/1/1)	2	0
07/02/06	10	6	3 (2/1/0)	0	
14/02/06	12	6	0 (6/0/0)		
15/02/06	12	10	3 (4/0/3)	0	
16/02/06	12	7	4 (1/0/2)	0	
22/02/06	12	11	0 (4/1/3)		
23/02/06	12	8	0 (6/1/1)		
28/02/06	12	7	2 (2/1/2)	0	
07/03/06	12	8	1 (2/5/0)	1	1
10/03/06	5	4	1 (3/0/0)	0	
15/03/06	8	4	1 (3/0/0)	0	
16/03/06	12	9	2 (0/3/1)	2	1
23/03/06	12	9	2 (7/0/0)	1	0
27/03/06	12	9	2 (5/2/0)	0	
30/03/06	12	10	0 (5/5/0)		
20/04/06	12	6	0 (3/2/0)		
26/04/06	12	7	0 (2/5/0)		
04/05/06	12	9	1 (4/4/0)	1	1
09/05/06	12	8	0 (1/7/0)		
01/06/06	12	10	0 (6/2/0)		
05/06/06	12	12	1 (10/1/0)	1	1
13/06/06	12	8	0 (0/0/0)		
11/07/06	12	9	1 (6/2/0)	0	
12/07/06	12	9	3 (3/2/1)	1	0
Totals	422	295	52(135/69/20)	12	5

There are 19 unaccounted for devices which failed in the non-ohmic stage.

Part 2 – Dielectric Spectroscopy of Carbon Nanotubes in Dichlorobenzene

Introduction

The second part of this project has been run in parallel with the nanowire project. This section starts with an introduction to the initial aims and literature in the field of a.c. electro-kinetic properties of carbon nanotubes. Following on from the introduction is an explanation of the experimental setups used and the results that were obtained. This section finishes with some explanations and ideas to explain the observations, a summary and then draws some conclusions.

Dielectrophoresis has been used by many groups to control and align nanotubes allowing their properties to be studied[33-35]. This technique can be used to create bundles of SWNTs which have applications, for example sensing gases[36]. Furthermore having nanotubes aligned across electrodes, intrinsic properties like the conductivity can be measured. This is usually done by lithographically contacting the ends of the nanotubes or by contacting them using micromanipulators or SPM methods[37-38].

Although there are many groups performing dielectrophoresis and managing to separate carbon nanotubes from solution there is no basic research into how nanotubes behave when suspended in solvent. The aim of this project is to suspend carbon nanotubes and perform dielectric spectroscopy on the solution. This should reveal more fundamental properties of nanotubes in applied alternating electric fields with the possibilities of observing the electric field strengths at which semi conducting nanotubes become conductors and even a way of measuring the conductivity of nanotubes. This information has direct application for dielectrophoresis by allowing groups to refine the frequency and magnitude of the fields that are used by a more scientific method than the trial and error approach that is currently employed.

Dielectrophoresis

Dielectrophoresis is the term used to describe the force on an induced dipole exerted by a non uniform electric field and is strongly dependent on the particles dielectric properties[39]. Dielectrophoresis itself is well understood and the mechanism behind the force exerted on a dipole is described below.

Consider a dipole which has a dipole moment $|\underline{p}| = qL$ where q is the charge on one end of the dipole (the charge on the opposing end is always equal and opposite –q) and L is the distance between the two charges.

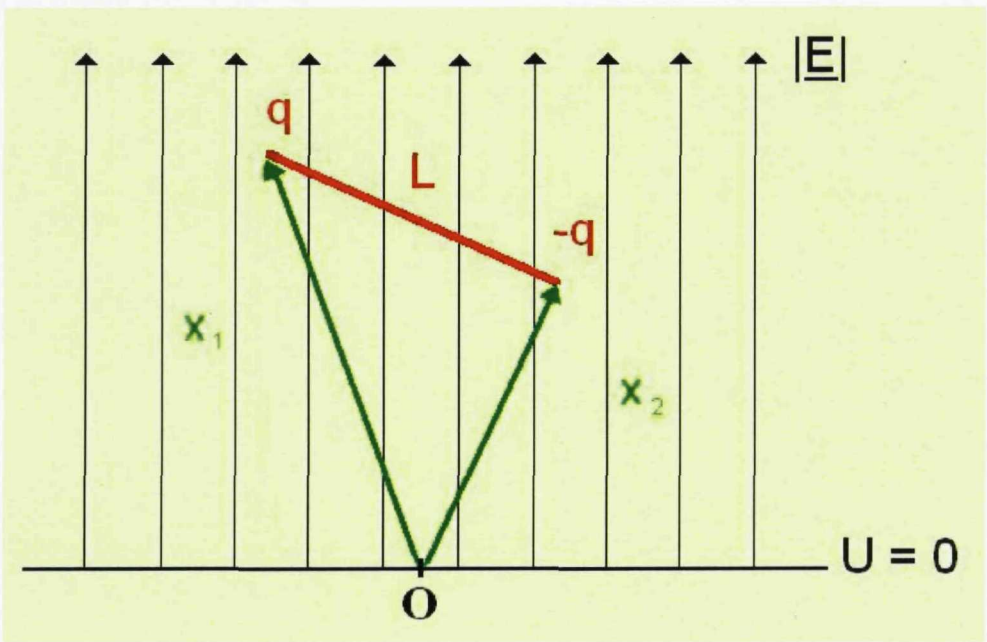

Figure 18. A dipole with magnitude qL in a uniform electric field magnitude $|\underline{E}|$. U = 0 denotes the arbitrary line of zero potential and $\underline{x}_1$ and $\underline{x}_2$ are the positions of the two ends of the dipole.

The electrostatic potential of the dipole is given by the sum of the potentials of the two charges

$$U_{dipole} = U_q + U_{-q} = -q\underline{E}.(\underline{x}_1 - \underline{x}_2) = -\underline{E}.\underline{p}$$

If instead of being in a uniform electric field the dipole is in a field with a spatially varying magnitude then assuming that a is positive, the standard case, then the dipole will be attracted to regions of high electric field magnitude where its energy is minimised. That is to say that it experiences a force given by

$$\underline{F} = \underline{\nabla}(\underline{E}.\underline{p})$$

In the case of dielectrophoresis the dipole is induced by the electric field. If we assume that the particle and its environment are isotropic then the induced dipole is given by

$$\underline{p} = \alpha \underline{E}$$

and

$$\underline{F}_{dielectrophoresis} = \alpha \underline{\nabla} |\underline{E}|^2$$

where α is the polarisability of the particle, and is controlled by the dielectric constant of the particle, the particles shape and the particles enviroment[40].

Clearly carbon nanotubes are not isotropic but are instead effectively long thin needles. Due to their shape they are much easier to polarise along their length than perpendicular to their length. This anisotropy means that in the presence of an electric field they experience a torque which tends to align them parallel to the field in the same way that a magnetic field aligns a compass. This torque is so strong that even in small fields nanotubes will quickly align along the field. In this case we can treat them as above with their polarisability being that for a field along the nanotube.

Preparing the solution

Before any measurements of nanotubes could be taken a suitable solvent that would allow the highest possible concentrations into suspension was required. Significant work was put in at the start of the project on different methods of suspending nanotubes in different solvents, the ideal solvent being non toxic and not needing to have all the experiments performed in a fume cupboard. Several groups work on suspending carbon nanotubes for various applications. Two common methods for suspending nanotubes were using isopropanol alcohol (IPA) or a solution of around 1% Sodium Dodecyl Sulphate (SDS) in water[39, 41, 42]. Bonard et al. saw aggregation of nanotubes in methanol, ethanol and acetone[42].

Both the IPA and SDS methods would have satisfied the criteria for toxicity and suspending nanotubes in both solutions was attempted despite the fact that SDS would alter the surface chemistry of the nanotubes. This was done by adding enough nanotubes to completely saturate the solution, then sonicating first with a 25kHz bench-top sonicator, then when that failed a 150 watt MSE ultrasonic disintegrator fitted with a 19mm horn probe. Following sonication the samples were centrifuged and the supernatant tested first in the impedance analyser and second imaged using an AFM. There was no success in suspending nanotubes either in IPA or with SDS and water so another solvent was required which could hold higher concentrations of nanotubes in solution[43]. Bahr et al. presented a table which shows the maximum concentration of nanotubes that can be suspended in given solvents[44]. Common solvents like acetone, methanol and ethanol can suspend less than 1mg/L. The top of the list was 1-2 dichlorobenzene which can suspend 95mg/L with chloroform second, able to suspend 31mg/L.

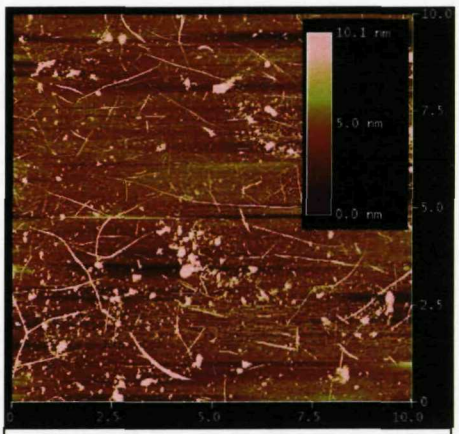

Figure 19. Atomic force microscope image of carbon nanotubes on a silicon oxide substrate

It is clear that 1-2 dichlorobenzene (1-2 DCB) is far better at suspending nanotubes than any other solvent tested. It is harmful and all stages of the sample preparation and measurement had to be performed under a fume hood but the gain in the amount of nanotubes suspended meant that this was the only option.

The nanotubes to be measured were suspended in 1-2 dichlorobenzene (1-2 DCB) by adding 10mg of single walled carbon nanotubes, produced by the HiPCO method purchased from Carbon Nanotechnoloies INC, to 10ml of 1-2 DCB. This was then sonicated in a 25kHz bench-top untrasonicator at maximum power for 15 minutes and centrifuged in an Eppindorf ultracentrifuge at 13,100g for 45 minutes. The supernatant could then be used for impedance measurements. Atomic force microscopy (AFM) images of the residual material from placing a drop of the supernatant onto an oxide coated silicon substrate and evaporating off the solvent were taken to check for the presence of nanotubes. An example image taken with a Digital Instruments Multimode AFM can be seen in Figure 19 which clearly shows the nanotubes. The concentration of the sample can be altered by taking the supernatant and diluting with 1-2DCB as required.

Experimental Setup

The aim is to be able to measure the dielectric properties of single walled carbon nanotubes suspended in a solvent. Throughout this project the basic method remained the same but there were refinements made as the need arose.

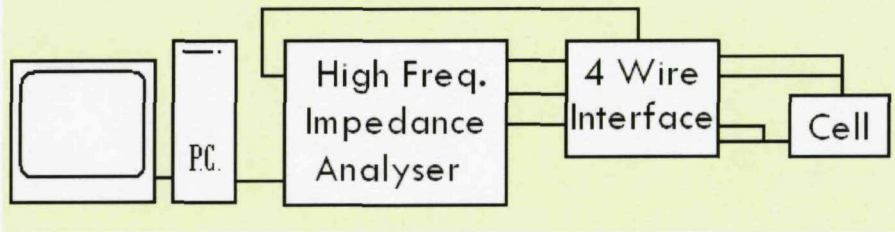

Figure 20. Diagram of the High Frequency Impedance analyser setup.

The basic setup is shown in figure 20. A Novacontrol Alpha A impedance analyser with a four wire test interface is connected to a measurement cell placed in a metal box which acts as a Faraday cage and screens external noise. There were two designs of cell used in the project, shown in figure 21. Originally there was a cylindrical design with steel electrodes coated with platinum black. Platinum black is both inert and very grainy which increases the surface area of the electrode and reduces the impedance caused by a charge double layer where charges collect close to the electrode surface leading to a capacitance. In this cell the two electrodes are separated by P.T.F.E. spacers. There were two major disadvantages with this cell. The first was that it only allowed for a two wire measurement, the second that it is possible that a charge layer could build up on the surface of the P.T.F.E. spacer leading to a parallel conduction path between the two electrodes. These two factors were shown not to have made a noticeable contribution when the experiments were repeated with the second design of cell.

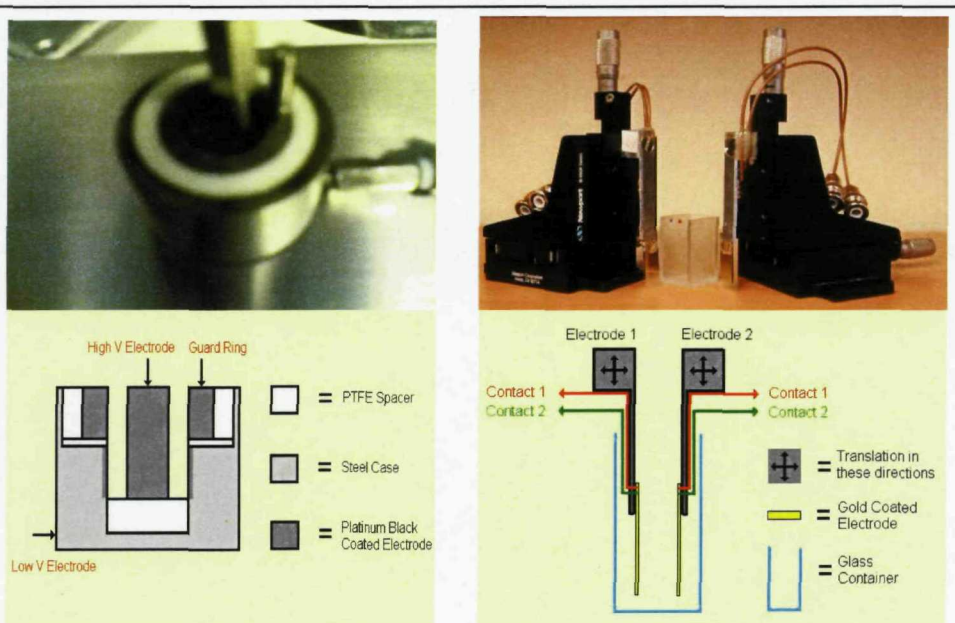

Figure 21. A) The cylindrical cell. **B)** The plate electrodes.

The idea for this second cell was to design a cell which allowed for the separation of the electrodes to be varied and had no possibility of parallel conduction pathways. This would allow experiments with a constant electric field and varying separation to be set up and remove any possibility that the observations are affected by factors other than the solution between the electrodes. The only disadvantage of this second design over the first is that it allows fringing fields to occur around the edge of the electrodes.

Fringing fields occur around the edges of the electrodes and are areas of weaker electric field outside of the volume between the plates. This effects measurements in two ways. The first is that the capacitance of the cell is not given by the simple equation $C = \varepsilon.A/d$ where A is the surface area of the electrodes and d is the electrode separation and ε is the permittivity of the dielectric between the electrodes. In a general case any non-linear effects will differ in areas of differing electric field strength. In our specific case the presence of non-uniform electric field could attract nanotubes to the area between the electrodes, increasing the concentration on nanotubes in the volume being measured. This effect will be minimised by having the separation between them much less than the minimum distance across the electrodes.

The electrodes themselves were made by cutting a glass slide to the correct shape and evaporating gold onto the surface to a thickness of 300nm using a 10nm chrome anchor layer, using an Edwards 304A thermal evaporator. Aluminium mounts were made such that the electrodes could be stuck facing each other and mounted onto a translation stage giving good control over their separation. The electrical connections to the electrodes were placed on the back of the mounts and connected to the feed-through on the faraday cage by co-axial shielded cable.

There are two kinds of measurements presented in this project, frequency spectra and time measurements. The frequency spectra are scans of varying the frequency, starting at high frequencies, typically 20MHz and ending at low frequencies typically 1Hz. The time measurements are taken at a constant frequency specified at the start of the measurement and the dynamics recorded over a set time. In both measurements the voltage and concentration can be changed as can the plate separation in the case of the plate electrodes.

Impedance Cell Theory and Cell Constant

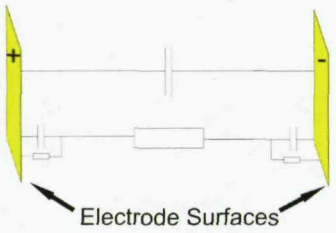

Figure 22. Simple model of a dielectric between electrodes.

A common method of understanding these cells is by using equivalent circuits. An equivalent circuit assumes that the cell responds linearly to electric field, which is the case if the a.c. electric field is small enough. Whilst this may not be true for all our measurements equivalent circuits are still a useful tool for interpreting our results. Equivalent circuits are a representation of a real cell made up from three components, resistors, capacitors and inductors. Figure 22 is the equivalent circuit we used to understand our results.

In figure 22 there are two separate conduction paths; the top path is the dielectric path and the lower path the ionic conduction path. The ionic conduction path represents any charge carriers in the system. The capacitor at the electrode surface represent the double layer capacitance, where a layer of ions can build up parallel to the electrode surface inducing an opposite charge on the surface of the electrode forming an additional capacitance. The resistor at the electrode surface represents an electrochemical reaction at the surface of the electrode. Under normal conditions the effect of the resistor and capacitor in parallel at the surface is very small compared to the total resistance or capacitance of the cell and can be ignored. The top capacitor represents the dielectric path where charge flow is due to the polarisation of the medium between the plates. As charge arrives on one plate the material between the electrodes polarises to neutralise this charge build-up. Consequently to keep over all neutrality charge must flow away from the second plate.

The Empty Cell

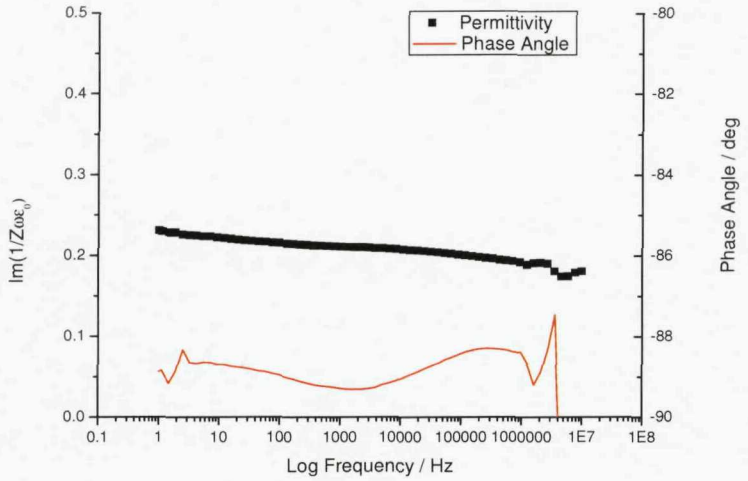

Figure 23. Result of a measurement with air as the dielectric between the plates where the permittivity is a plot of the measured permittivity, not factoring the cell constant at 1.0V.

The plot in figure 23 shows the results of a measurement with no solution between the plates, i.e. the dielectric medium is air. As expected both the phase and $1/Z\omega\varepsilon_0$ (see below) are approximately constant regardless of the frequency. The phase remains close to -90 degrees throughout the measurement, as it should, for a capacitor. In measurements with a solvent between the electrodes the response shows a rise in phase to 0 degrees and the value of impedance to tend to a constant for decreasing frequency at low frequencies. This measurement of air demonstrates that such response is due to ions in the solution and is not a property of the cell or the analyser used for the measurements.

Cell Constant

As previously mentioned the capacitance of an infinite parallel plate capacitor is given by the equation $C = \varepsilon.A/d$. In this case the cell constant is the area of the plates divided by the distance separating them. In reality plates are not infinitely large, however C remains proportional to ε and the constant of proportionality relating them is the cell constant k. The equation describing the capacitance becomes $C = \varepsilon k$.

The resistance of the cell due to ionic conduction is also related to its bulk value in the material between the plates, resistivity, by the cell constant and is given by $R = \rho/k$ where ρ is the resistivity. In parallel plate cell the charge flow through the bulk material due to C and R scale linearly with k, but surface effects do not scale in the same way. This allows a cell to be designed such that the surface effects are minimised, which as mentioned is done by keeping the distance between plates much less than the distance across them.

The cell constant of a real life cell can be estimated using simple theories, however not accurately determined. To determine the cell constant it must be measured. To do this different samples of known permittivity are put between the plates of the cell. It is assumed that there is no ionic conductivity as would be the case with a perfectly pure solvent. The impedance is then measured and in this case with no ionic conductivity hence no associated parallel resistance the impedance is directly related to the capacitance given by;

$$Z^* = \frac{1}{j\omega C} \equiv \frac{1}{j\omega \varepsilon k}$$

By measuring Z, the permittivity multiplied by the cell constant can be determined and is given by the imaginary part of $1/Z\omega\varepsilon_0$.This value is then plotted against the known permittivity for the sample. When this is done for a number of different samples the slope of this line is k, the cell constant.

Determining the Cell Constants Experimentally

As well as determining the cell constants these tests also acted as control experiments to show that the set-up yielded consistent results. The permittivity of the solution in the cell is ascertained by plotting $Im(1/Z\omega\varepsilon_0)$ as a function of frequency. At high frequencies this values tends to a constant, an example of which is shown on the below labelled figure 24.

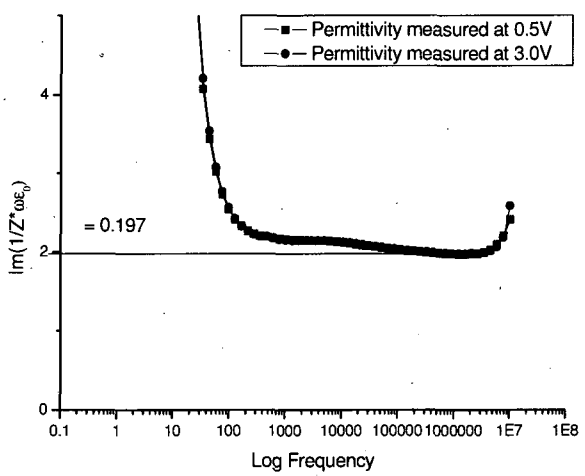

Figure 24. Example of a plot of permittivity times cell constant as a function of frequency. This is from the plate electrodes at 2.0mm separation using IPA and the point appears on figure 26A below.

Note that the value of $Im(1/Z\omega\varepsilon_0)$ rises sharply at high and low frequencies. At the very high frequencies this is an instrument effect. The measurement starts at high frequencies and the first points are skewed as the set-up settles down. To eliminate this effect the measurement could have been repeated scanning from low to high frequencies, however this was not considered at the time and in

reality does not have a bearing on the results. At low frequencies the impedance of the dielectric path gets very large, therefore the charge carriers present in the medium becomes the dominant method of charge transport across the cell, invalidating the neglect of the ionic path in the equation. For these reasons the value of $Im(1/Z\omega\varepsilon_0)$ is taken at as higher frequency as possible before instrument effects begin. In practice it is the point where the value is at a minimum.

Both cells have had their cell constant determined in this way. For the plate electrodes the cell constant was determined at different plate separations and when the measured cell constant is plotted against the inverse of the separation the expected straight line appears, from which the cell constant at any separation can be read, see figure 26.

For the cylindrical cell the solvents are, in increasing permittivies, air, o-dichlorobenzene, isopropanol alcohol, acetone and methanol. Methanol is not included in the final calculation of the cell constant as it does not give a reliable result as it readily picks up ions and absorbs water from the atmosphere. This means the parallel resistance term is never negligible and the permittivity does not tend to the correct value with increasing frequency.

As can be clearly seen the best fit line on figure 25 does not pass through the origin as should be expected. This is due parallel capacitance paths present in the cylindrical cell with the electric field passing through the PTFE spacer. This capacitance will be constant through out our experiments and its effect can in principle be subtracted from all the data. However as all our conclusions concerning the data are made via qualitative comparisons and for many measurements, particularly of activated nanotube samples, the fixed capacitance is effectively short circuited by the sample impedance we have chosen to present the raw impedance data throughout instead of presenting partially processed data. However the effect of the parallel capacitance should be born in mind when considering any data taken in the cylindrical cell. For all measurements presented the cell used to obtain them is given.

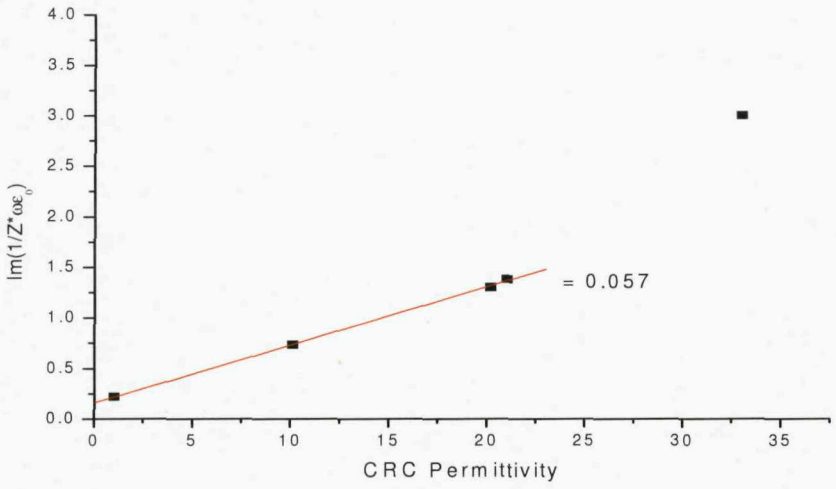

Figure 25. Determination of the cell constant of the cylindrical cell.

The solvents used for the plate electrodes are, in increasing permittivity, hexane, toluene, chlorobenzene, o-dichlorobenzene and isopropanol alcohol. These measurements conclusively show

that the set-up works and measures different solvents proportionally. This in turn strongly suggests that the data acquired is due to the properties of the solvent itself and not an effect of the equipment. Note the missing data point on Figure 26A for toluene with a 2.0mm gap. This is because after analysis the result was revealed to be highly anomalous. The test should have been repeated however a good fit to the points was still possible.

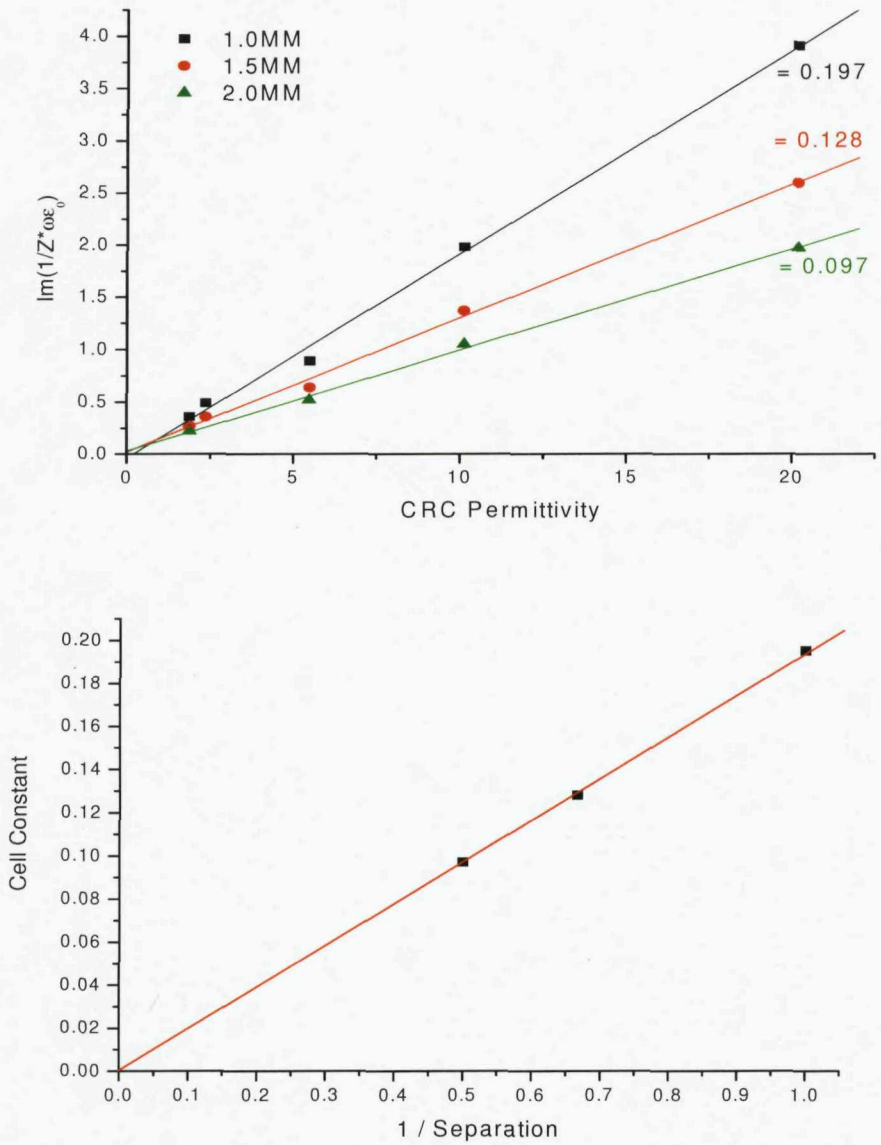

Figure 26. **A)** Im($1/Z\omega\varepsilon_0$) of solvents versus known permittivities at different separations. **B)** Cell constant vs. 1/Separation

Results

Before it is possible to characterise the behaviour of the carbon nanotubes suspended in dichlorobenzene it is necessary to understand how the dichlorobenzene itself responds to an applied a.c. electric field. To achieve this plain 1-2 dichlorobenzene (DCB) was measured with different voltages, frequencies and plate separations. Fresh solution form the same overall batch was used each time and the electrodes rinsed with DCB and dried with compressed air between each measurement.

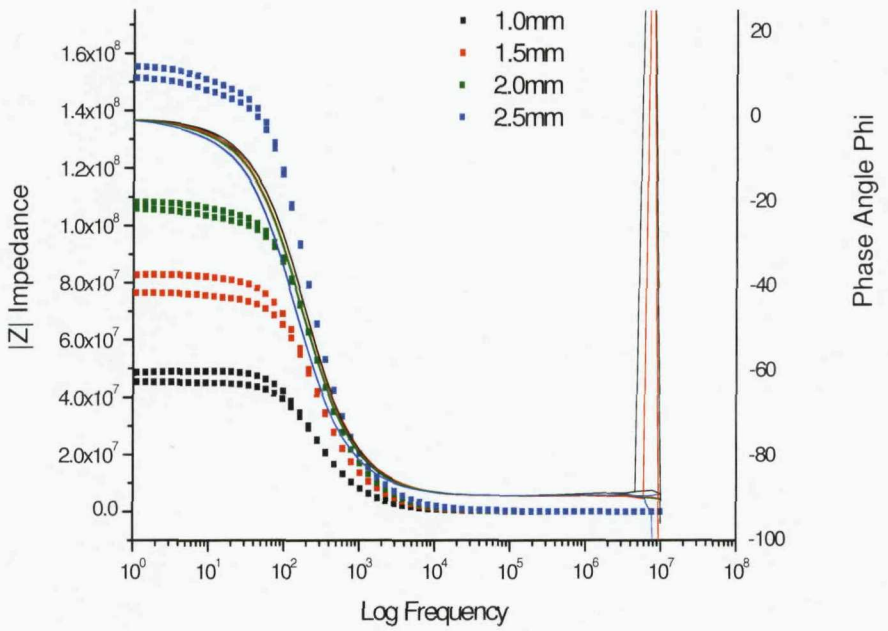

Figure 27. Shows the response of plain o-dichlorobenzene according to varying voltage and plate separation. The solid lines correspond to the phase angle and the dashed lines correspond the magnitude of the measured impedance. In each pair of measurements the higher impedance is associated with the lower voltage.

Some representative results of plain Sigma Aldrich CHROMASOLV grade DCB are shown in figure 27. The first point to mention is the anomalous data at the very highest frequencies is an artefact of the analyser as it begins its measurement. It is shown in this figure for completeness but is disregarded in all further figures. The form of the response is as expected from the theory mentioned in the previous section. At high frequencies the impedance due to the dielectric path is low and this is therefore the dominant method of current flow which results in a phase shift of -90 degrees between the voltage and current as would be expected from a capacitor. As the frequency drops this impedance rises and the ionic conduction path becomes the dominant method of current transport across the cell until at the lowest frequencies the impedance due to the dielectric path is extremely high so all the current transport is via the conduction path, the impedance of which has a zero degree phase shift.

The results shown in figure 27 were taken with different plate separations and they show that as the gap between the electrodes increases the impedance of the conduction path increases. From these results it is possible to calculate the resistivity of DCB using the cell constant read from the graph labelled Figure 26B and assuming that the impedance at low frequencies is entirely due to the resistance of the ionic path. From the 4 results, using the low voltage plot in each case, the average resistivity was found to be $1.007 \times 10^7\ \Omega m^{-1}$, with a standard deviation of $9.66 \times 10^5\ \Omega m^{-1}$. The high frequency response was used to calculate the values of $Im(1/Z\omega\varepsilon_0)$ for DCB at different separations shown in figure 26A. The fact that these values are on the line obtained from the other calibration solvents indicates that the dielectric constant of DCB is as expected.

A further obvious effect here is the difference in the impedance for different voltages at the same separation. It should be said that this effect is small, much smaller than changes caused by the presence of nanotubes. However this splitting is an example of a nonlinear effect. It only occurs at low frequencies so the effect must be due to the ionic conduction path. Furthermore the splitting is constant even though the electric field strength is varied by changing the distance between the plates. The effect is only dependent on the amplitude of the applied ac potential difference, which strongly suggests it is a surface effect. In this case it is most likely to be the presence of electrochemical reactions at the electrode surface. In general the rate of an electrochemical process varies exponentially with applied potential over some threshold and thus as the potential is increased the current flowing via this reaction will increase and the resistance corresponding to this process will decrease.

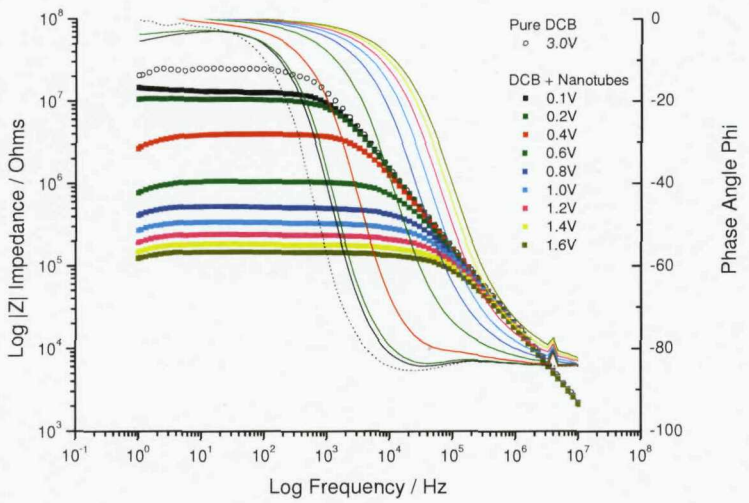

Figure 28. Response of nanotubes in DCB as the voltage is increased. The fine solid lines correspond to the phase angle and the thick lines the measured impedance. Plain DCB is included with the impedance shown as unfilled circles and the phase as the dashed line. Note the two order of magnitude drop in impedance with increasing voltage and the corresponding higher frequency phase transitions.

Once the DCB had been studied, carbon nanotubes could be added and a similar experiment carried out; see Figure 28. The salient feature of figure 28 is that it shows that nanotubes present in the

solution significantly change the result of the measurement. Even at very low a.c. amplitudes the presence of nanotubes lowers the impedance by a factor of two, which is large compared to any changes observed in plain DCB, the largest of which was a lowering of the impedance by a factor of 8% when 3.0V was applied. As the amplitude of the potential is raised the impedance continues to decrease until it saturates and no further decrease is observed. In this experiment this point occurred at an applied amplitude of 1.6V at which point the impedance had decreased by two orders of magnitude. It should be noted that as voltage is increased in this experiment the time which the suspension of nanotubes has been subjected to a potential difference has also increased. This proves to be important and is discussed later on in this section.

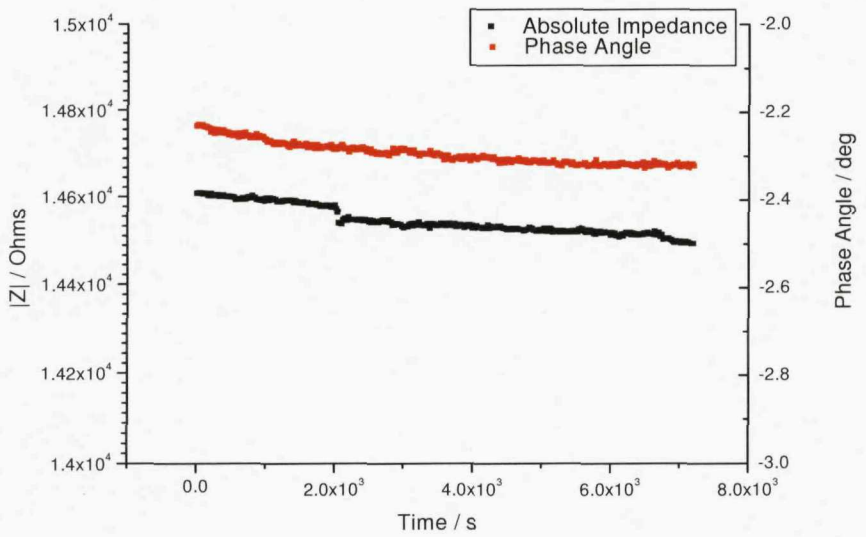

Figure 29. Time dynamics of a sample which has been subjected to a high voltage. Measurements were taken at an intermediate frequency at low voltage in an attempt to quantify any decay to the samples original state.

A measurement at 0.1V immediately after the sample has been "activated" by applying a high a.c. potential gives the same result as the high potential. This means that any changes induced by the higher potential are at least semi-permanent. The next experiment was to determine whether the observed drop in absolute impedance was permanent. If it were temporary it would be expected that the value for impedance would revert to its original value at low voltage after a period of time. The experiment was performed in the cylindrical cell by measuring at an intermediate frequency of 10^4 Hz at a low voltage over a period of 2 hours, with a measurement point taken every 20 seconds. The frequency used was chosen taking into account the results presented in figure 28. That is to say an intermediate frequency was chosen so that both the magnitude and phase of the impedance should be sensitive to any relaxation. Figure 29 shows that if the system was reverting to its original state, then the process was very slow. It also shows that the absolute value of impedance is still falling albeit very slowly. If this were a genuine decay to the original state then the impedance value should be rising

slowly back towards its original value. This leads to a conclusion that no decay over time can be observed and that the change in the solution is stable over extended periods.

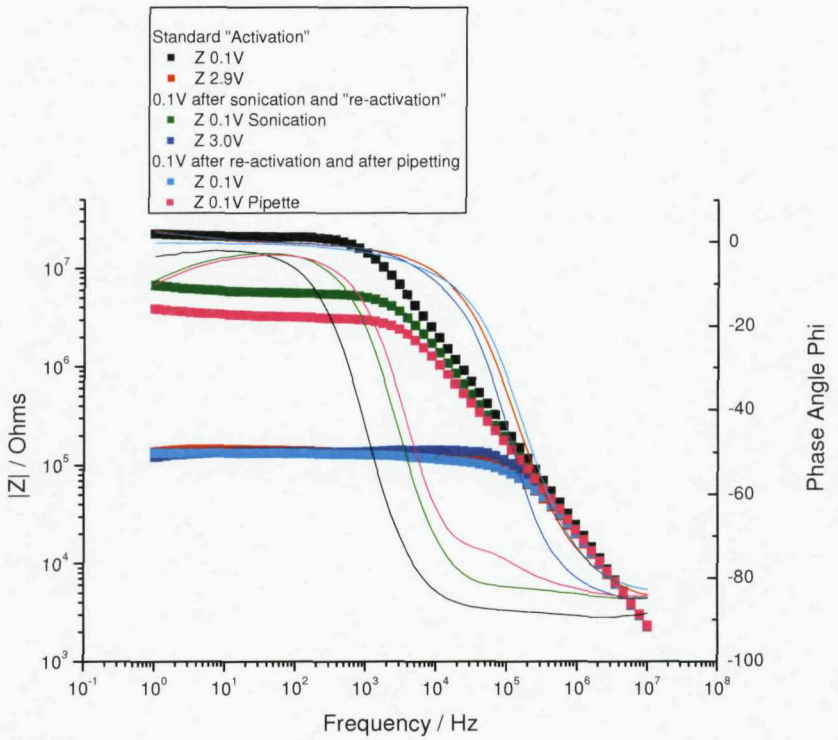

Figure 30. This plot shows the results of the experiment of removing the solution and re-measuring in the order going down the list in the legend. The solid lines are phase and the lines constructed of points show the absolute impedance. The sample was measured at low applied voltage and then activated with 3.0V. The sample was removed and sonicated, then re-measured at low voltage. Finally it was re-activated and the effects of removing and replacing with a pipette determined.

The next experiment was to quantify whether the change was a chemical change in the solution or if it was an alignment or interaction between the nanotubes. The sample was removed from the cylindrical cell, sonicated for 10 seconds and then re-measured. Next the sample was activated and then removed and replaced with a pipette to examine if a more gentle disturbance had the same effect. Between each measurement the electrodes were rinsed with DCB and dried with compressed air.

The results of these experiments are shown in figure 30 and were performed in the order of the legend. All the curves are of nanotubes suspended in DCB. The first measurement was performed at 0.1V (black) showing the response at low frequency. The second measurement at 2.9V (red) gave the expected activated impedance. Immediately after this measurement the sample was removed and sonicated for 10s and then re-measured at 0.1V (green). This measurement showed a significant return towards the original state, which would not have been observed if the sample had not been disturbed.

The sample was returned to the low impedance state by measuring at 3.0V (blue) and then checked by measuring at 0.1V (cyan) to confirm that when undisturbed a low voltage measurement after the sample has been put into the low impedance state, will still show a low impedance. The sample was then taken out with a pipette and returned to the cell and measured at 0.1V (purple) revealing a return towards the original higher impedance state. This experiment clearly shows that physically disturbing the sample reverses the activation, where sonication is more effective than simply pippetting. However even sonication does not completely return the sample back to its original state. This strongly suggests that activation involves some form of aggregation of nanotubes and that some fraction of these aggregates are strongly enough bound together to stay together when sonicated.

The following set of experiments were undertaken to get an understanding into the dynamics of the formation of the "activated" state. Three separate sets of experiments were performed to determine the effect on the dynamics of a single variable; a) ac amplitude, b) nanotube concentration and c) frequency. In each case the magnitude and phase of the impedance was measured at a specific frequency. The experiments were performed in the cylindrical cell. The results of these experiments are shown in figures 31 a-c. The captions associated with Figures 31 a-c refer to concentrations 1, 2 and 3. As determining the absolute concentration of nanotubes suspended in any particular sample is very time consuming and difficult it was decided to use a relative concentration scale. The stock solution was produced in a similar manner to that discussed in reference 43 and as such is likely to have a concentration of 95mg/L[43]. Concentration 1 will be approaching this value. Concentration 2 is diluted by a factor of 2 and concentration 3 is diluted by a further factor of two. This makes the relative concentration of concentration 1 equal to 1.0, concentration 2 equal to 0.5 and concentration 3, 0.25 that of concentration 1.

As shown in figure 31a the response happens faster as the amplitude of the ac potential is increased. This might be expected if aggregation is responsible for the activation. The strength of the dipoles on the nanotubes increases linearly with amplitude of ac potential and the force of the interaction between dipoles increases with the magnitude of the strength of the dipole squared.

As shown in figure 31b the response is fastest when the concentration is highest. Aggregation requires that particles come close to each other which occurs more often if there is a higher concentration. A naïve prediction would be that the rate of the formation of the activated state would be proportional to the concentration squared.

The frequency experiment, the results of which are shown in figure 31c is much harder to understand. This is because at different frequencies current flows across the cell via different methods meaning that the measurement is being taken with the same variable that causes the observed changes in impedance and phase. The absolute impedance values for the different frequencies appear to cross over in the first few seconds on figure 31c. This is unexpected but due to the similar values for impedance at these frequencies then any small difference in the initial conditions of the cell might account for this before the measurement settles.

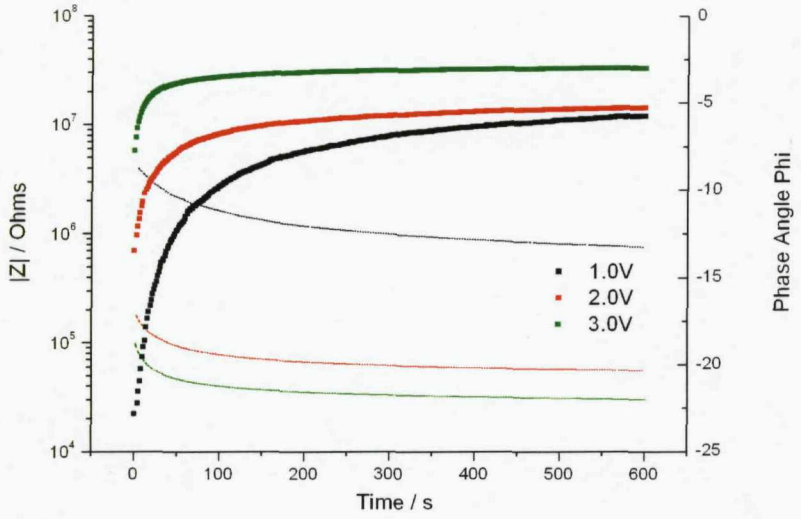

Figure 31a. Plots of time dynamics for varying voltage. The impedance is shown as the fine line and the phase the thick line. This measurement was performed at 1 x 10^4 Hz at concentration 2 (See caption for figure 31b for explanation of concentrations).

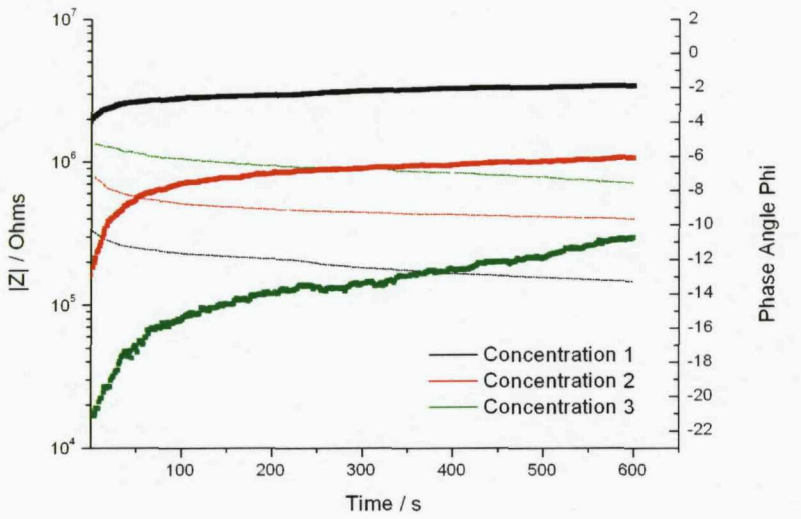

Figure 31b. Plots of time dynamics for varying concentration. Impedance is shown as the fine line and the phase the thick line. These measurements were performed at 1 x 10^3 Hz at 3.0V. Concentration 3 is half that of concentration 2, which is half that of concentration 1. For estimates of the concentrations see text on page 52.

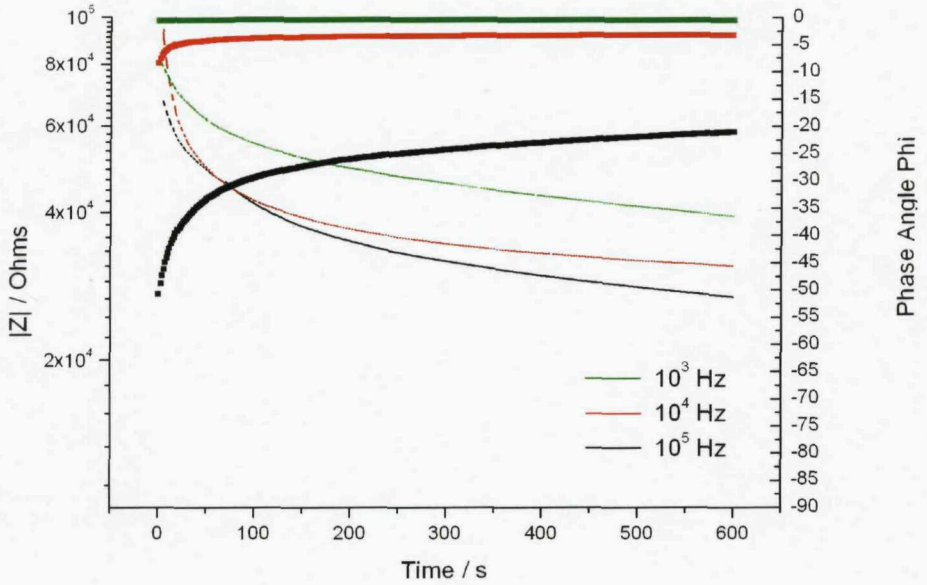

Figure 31c. Plots of time dynamics for varying frequency. The impedance is shown as the fine line and the phase the thick line. This measurement was performed at 3.0V using concentration 1.

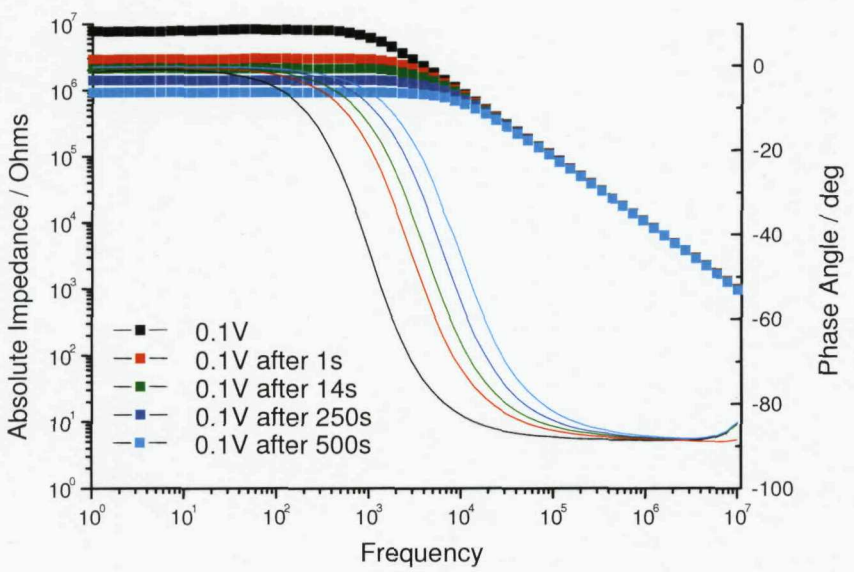

Figure 32. Frequency spectra after sample has spent time being measured at 3.0V. The solid lines show the phase angle and the dotted lines show the absolute value of the impedance. The experiments were performed in the order shown in the legend with the times showing how long the sample had spent at 3.0V applied at 1 x 10^3 Hz

Following on from the time dynamics experiment presented above, the next stage was to use these results to pick a set of times to apply a 3.0V potential to the samples. Following this activation the frequency dependent impedance of the samples was measured at 0.1V using the plate electrodes. This was achieved by using the original time spectra, figure 31a, to pick points where the value of the phase had dropped to half its previous value. The results of this experiment are shown in figure 32 and are roughly as expected, with each increase being the same as the previous one. The results after 500 seconds are at a slightly higher frequency than may have been expected if the phase was constant after 250 seconds as shown in figure 31a, nonetheless the change from dielectric to resistive behaviour has not shifted up in frequency by as much as it did in the first 250 seconds.

Following each result in this section is a brief discussion on what type of physical effect could give rise to the observations. In most cases this leads to the idea of nanotube aggregation or alignment as a method of explaining the data. As an additional test of this concept Atomic Force Microscopy using a Nanosensors Multimode III atomic force microscope was performed on samples prepared using a nanotube solution both before and after the "activating" a.c. field had been applied. It was expected that once nanotubes were aggregated they would not come apart easily and if this were the case then an increased proportion of bundles would be visible.

The sample was prepared by taking up 100µl of solution carefully into an Eppindorf pipette and depositing onto a $5mm^2$ silicon substrate, which had been cleaned by sonication for 30 minutes in IPA and blown dry with compressed air. The sample is then left in a fume hood for the DCB to evaporate, depositing the nanotubes onto the surface to be imaged.

There were two samples prepared in this was on different days, named 0109 and 0209. Each of these had two samples prepared for imaging, one using solution before "activation" and one from the same batch of solution after. This resulted in 4 AFM images fit for analysis and an example of each of these with a representative line scan are shown below.

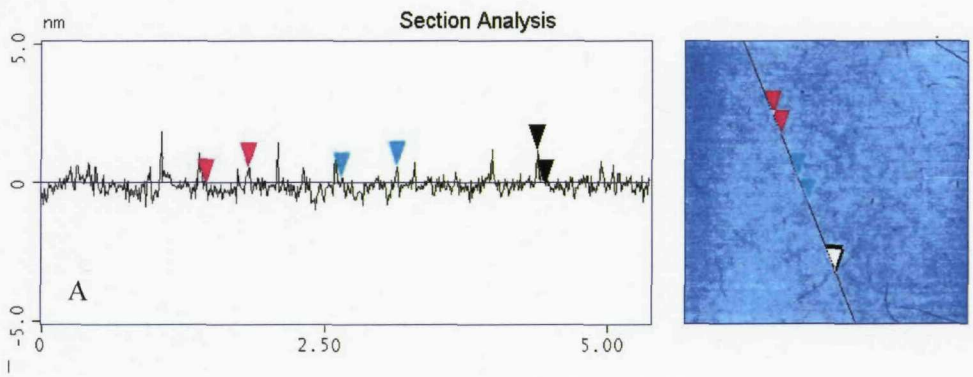

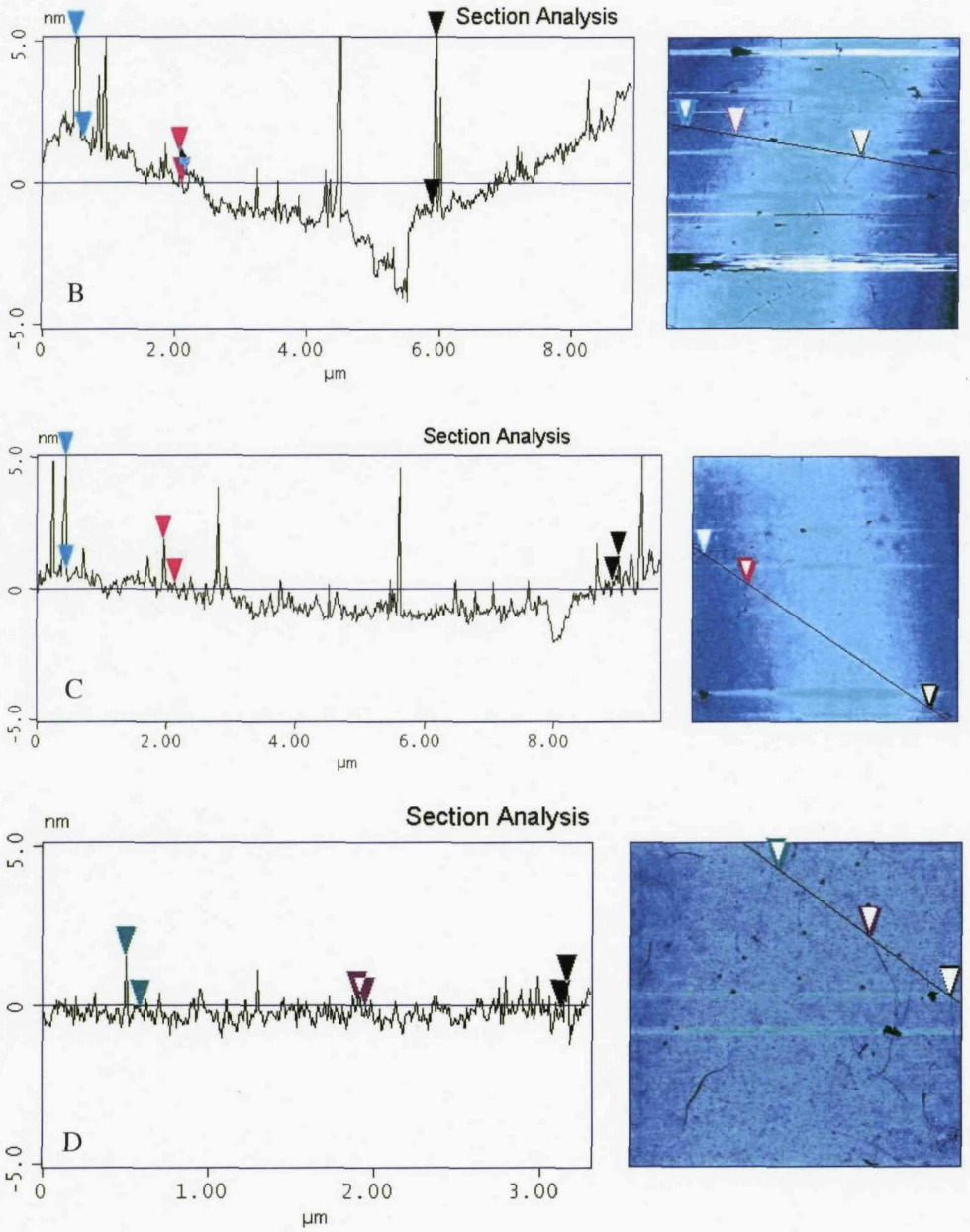

Figure 33. A and B show the images and example line profiles from 0109 and 0209 respectively, without and a.c. field applied. C and D are 0109 and 0209 after "activation" had been observed.

Line profiles through the images were analysed in order to determine the nanotube diameters. The results show the average nanotube diameter measured before and after activation and the percentage of measured nanotubes below 3nm in diameter for each sample. Whilst there is no fixed value for the diameter of a single walled carbon nanotube anything that measures greater than 3nm can reasonably be expected to be an aggregate of more than one nanotube. The following table summarises the results.

	0109 before	0109 after	0209 before	0209 after
Average nanotube diameter / nm	2.40	3.13	3.14	2.12
Percentage of visible nanotubes below 3nm diameter / %	60%	50%	60%	60%

The results here are not conclusive. They show no significant difference between before and after over the samples. There could be a number of reasons as to why this is the case. First, it is difficult to measure the smallest of nanotubes, as can be seen by the pink measurement markers in figure 33 A – D. This could mean that the individual nanotubes are miscounted. In principle this means that the ratio of bundles to tubes may not be well defined. Aside from the measurement difficulties the way the samples were prepared could give rise to the observed same result for before and after. Despite considerable efforts to remove aggregates from the samples by sonication and centrifuging aggregates are still observed in the AFM data for the sample before activation. It is possible that the nanotubes are aggregating during the drying process and whist alternate drying mechanisms could have been investigated the time was not available for this experiment. Ultimately this would have been an excellent confirmation of the suspected mechanism behind the observed results. Whilst this experiment is inconclusive the alignment/aggregation model still seems to the best available model to explain the other results.

Conclusions

It has been demonstrated that the measured dielectric response of plain DCB is largely as expected with only a very small dependence on amplitude of a.c. field applied likely to be due to electrochemical reactions at the electrode surfaces. It has also been shown that suspending nanotubes in the DCB lowers the impedance at low frequencies significantly even when measured with very low amplitude a.c. field. The response of the suspension at high frequencies remains unchanged from that of plain DCB. Applying a larger amplitude a.c. field results in an activation of the sample where this low frequency impedance is decreased by as much as two orders of magnitude. This activation is at least semi permanent as re-measuring with a small a.c. field, even after two hours, results in the same response as that of the measurement with a large field. The only way found to return the sample back to a non-activated state was by mechanically disturbing it. The more vigorous the disturbance the further toward its original state the sample returned, although even with sonication the sample never completely reverted all the way back to its original response. The activation dynamics were found to depend on amplitude of the applied field, with larger amplitudes activating the sample more quickly, the concentration of nanotubes suspended in the DCB, with higher concentrations resulting in faster activation. An attempt was made to see frequency dependence but no strong correlation was observed and deficiencies in the setup make it difficult to draw any conclusions.

Although it is possible that there are alternative explanations for the results presented in this project, aggregation of the nanotubes does fit with all observations and is made particularly convincing by the results of physically disturbing the sample. In principle chain formation is known in dielectrophoresis[39, 40]. It has been well researched experimentally particularly in the field of electro-rheological fluids where applying an electric field alters the viscosity of the fluid[39] and has even found widespread commercial application including adjustable damping in automotive suspension systems. Furthermore, once the nanotubes have come together Van der Waals forces will keep them together even when the electric field is removed; neatly explaining why the system does not revert back to its original behaviour after the field is switched off.

Chain formation occurs as the positive end of one dipole and the negative end of a second dipole are attracted to each other. However the dipole field drops off $1/r^3$ and the force between the dipoles falls as $1/r^4$, so for chain formation to occur there must be a high enough concentration of dipoles such that on average they are close enough to feel an attractive force from each other. Once the dipoles come together they interact to form chains with the direction of the overall net dipole depending on whether the individual particles are more or less polarisable than the medium. If the particles are more polarisable then the dipoles align parallel with the electric field, if they are less so then the dipoles align anti-parallel. Particles with different polarisability with respect to the medium are still attracted to each other, except these will chain perpendicular to the field lines as opposed to parallel with like particles[45].

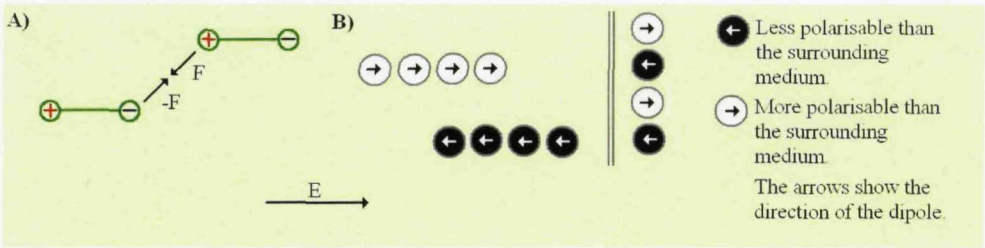

Figure 34. A) The attractive force on a dipole that causes chaining. **B)** Modes of chaining for particles with different polarisabilities with respect to the medium they are suspended in.

There are many different types of nanotube characterised by their chiral vector and each of these will have a different polarisability. Indeed some nanotubes are conducting and other are semi-conductors depending on their configuration and the situation with nanotubes becomes even more intractable when a reason into why chaining changes the dielectric properties of a material is considered.

Understanding why aggregation of particles decreases the impedance is more difficult. Theory has been calculated for the simplest case which is the chaining of spheres[39]. The result of this theory is that the effective permittivity of a particle increases proportionally to N^3 where N is the number of particles in the chain. However the number of individually contributing structures decrease proportional to 1/N as the chains grow. This means the total effective permittivity of the solution increases proportional to N^2 assuming all the chains are of equal length. Additionally when the particles are closer than their radii multipolar interactions must be considered which further alter the effective permittivity the chains.

Extending even the simpler chaining theory to nanotubes would be extremely difficult, way beyond the scope of this project and at the time of writing no such theory exists for a number of reasons. First the nanotubes are not spheres but very long thin needles. Secondly there are many different types of nanotube and any theory would have to take into account the interaction between any given pair. Furthermore preferential chaining and the influence of chaining on the different types of nanotube would have to be considered and finally the interaction between particles depends critically on the position of the ends of the particles. Unlike spheres that can only contact in one way nanotubes can contact in many different configurations with differing amount of overlap or wrapping.

In conclusion the experimental evidence, although indirect suggests that aggregation of carbon nanotubes in the DCB is responsible for the observed drop in impedance at low frequencies. A direct observation of nanotube chains would be the final support for the chain formation hypothesis. Whilst an attempt was made using AFM to obtain this evidence the results were inconclusive. Worryingly aggregated nanotubes were observed when the non-activated solution was dried onto a substrate. As standard procedures were used to obtain non-aggregated nanotubes in the solution it is not clear how these aggregates formed but it seems likely that it was during the drying process. Thus it appears that the AFM measurements as we performed them are unable to provide the evidence we require. It should

be noted that without the direct evidence of chain formation it is not possible to be absolutely certain that chain formation is the activation mechanism however it remains the most plausible.

Overall Conclusions

The first part of this project was to measure the electronic properties of small numbers of molecules by introducing them to a gapped gold nanowire which had been contacted using photolithography. Results from this part of the project were difficult to come by due to the process having a large number of challenging practical steps required to complete a device. The project does demonstrate that the idea can work but significant improvements must be made to the total yield of completed devices before it becomes an efficient use of time. However by the end of the project there were still many ideas on how to improve the yield. One of these ideas was based on a result observed very late on in the project regarding nanowires snapping as they are released from the membrane in which they were grown. A sensible next step would be to confirm this result and look at methods to reduce or eliminate the problematic sonication stage, perhaps by using a different track etched membrane, for example a polycarbonate membrane which readily dissolves in dichloromethane. If the wires snapping is the problem some of the results seem to suggest, then if it could be overcome the yield might increase dramatically making the technique viable. Further ideas centred on using dual layer resists to achieve more accurate device fabrication or miniaturising the method and using e-beam lithography. E-beam lithography would allow smaller diameter wires to be contacted, which in turn allows the wires to be grown to a shorter total length meaning they will be more robust to the fabrication steps.

In my opinion the idea behind this project is a good one, which is a large part of the reason why I took on the project. I do not believe it was a complete failure and think that if even one of the ideas to improve the wires or fabrication paid off the method could quickly start to produce results in the numbers that were hoped for originally.

The second part of the project set out to discriminate between nanotubes with different band gap energies to aid in their separation by dielectrophoresis. It was discovered that it was possible to measure the effect of nanotubes in a solvent by impedance spectroscopy and that by increasing the electric field strength caused the absolute impedance to decrease by two orders of magnitude. This decrease was not a simple relation to field strength but saturated to a point where no further decrease could be observed with the field strengths we were able to apply. It was found that the rate at which the system reached this threshold depended strongly on the magnitude of the field applied and concentration of the nanotubes suspended in the solvent, with the higher the field or concentration the faster the system reached its lowest impedance. This change in impedance was at least semi-permanent with no decay recorded over a very long measurement period. Further work found that by disturbing the sample the impedance of the system could be made to revert back towards its original higher value and that the more vigorous the disturbance the closer to the original value it became. This result led to the overall conclusion that it was an alignment or aggregation of the nanotubes that caused the observed drop in impedance, although a detailed mechanism of how this is caused is still not certain.

To continue this project it would be a good experiment to attempt the same measurements but with a micrometer scale gap between the measurement plates. This would allow individual nanotubes to completely bridge the gap and allow an accurate conductivity for nanotubes to be determined. Further work on directly imaging the nanotubes in the two states should be carried out and if this could

be achieved would add considerable weight to the conclusions. Overall this project is very promising with good, unexpected results forthcoming and plenty of scope for continuation both with the experimental side on achieving the ultimate goal of separating out the different nanotubes and the theoretical side of understanding the mechanism which causes the impedance to decrease.

References

[1.] C. E. Gardner, M. A. Ghanem, J. W. Wilson, D.C. Smith, Development of a Nanowire-Based Test Bed Device for Molecular Electronics Applications, *Anal. Chem*, 2006, vol 78, pp 951-955

[2.] Brent A. Mantooth and Paul S. Weiss. "Fabrication, Assembly, and Characterization of Molecular Electronic Components." *Proceedings of the IEEE*, Vol. 91, No. 11, November 2003.

[3.] R. E. Holmlin, R. Haag, M.L. Chabinyc, R.F. Ismagilov, A.E. Cohen, A. Terfort, M.A. Rampi and G.M. Whitesides. "Electron transport through thin organic films in metal-insulator-metal junctions based on self assembled monolayers," *J. Amer. Chem. Soc.*, vol. 123, pp 5075-5085, 2001.

[4.] Y. Selzer, A. Salomon and D. Cahen. "Effect of molecule-metal electronic coupling on through-bond hole tunnelling across metal-organic monlayer-semiconductor junctions," *J. Amer. Chem. Soc.* Vol. 124, pp 2886 – 2887, 2002.

[5.] Y. Selzer, A. Salomon and D. Cahen. "The importance of chemical bonding to the contact for tunnelling through alkyl chains," *J. Phys. Chem. B*, vol 106, pp 10432 – 10439, 2002.

[6.] I. Amlani, A. M. Rawlett, L. A. Nagahara, and R. K. Tsui, "An approach to transport measurements of electronic molecules," *Appl. Phys. Lett.*, vol. 80, pp. 2761–2763, 2002.

[7.] J. G. Kushmerick, D. B. Holt, J. C. Yang, J. Naciri, M. H. Moore, and R. Shashidhar, "Metal-molecule contacts and charge transport across monomolecular layers: Measurement and theory," *Phys. Rev. Lett.*, vol. 89, 2002.

[8.] J. Shen, G. Kramer, S. Tehrani, H. Goronkin, and R. Tsui, "Static random-access memories based on resonant interband tunneling diodes in the InAs/GaSb/AlSb material system," *IEEE Electron Device Lett.*, vol. 16, pp. 178–180, May 1995.

[9.] S. Gregory, "Inelastic tunnelling spectroscopy and single electron tunnelling in an adjustable microscopic tunnel junction." *Phys. Rev. Lett.* vol 64, 689 (1990)

[10.] P. Samori, J. P. Rabe, Scanning probe microscopy explorations on conjugated (macro)molecular architectures for molecular electronics, *J. Phys. Condens. Matter*, 2002, vol 14, 9955 - 9973

[11.] Wolfgang Haiss, Harm van Zalinge, Horst Ho¨benreich, Donald Bethell, David J. Schiffrin, Simon J. Higgins, and Richard J. Nichols, "Molecular Wire Formation from Viologen Assemblies," *Langmuir*, 2004, vol 20, 7694 - 7702

[12.] L.A. Bumm, J.J. Arnold, M.T Cygan, T.D. Dunbar, T.P. Burgin, L. Jones II, D.L. Allara, J.M. Tour, P.S. Weiss. "Are singular molecular wires conducting?" *Science*, 271, March 1996

[13.] T. Ishida, W. Mizutani,, N. Choi, U. Akiba, M. Fujihira, and H. Tokumoto, "Structural Effects on Electrical Conduction of Conjugated Molecules Studied by Scanning Tunneling Microscopy," *J. Phys. Chem. B* 2000, vol. 104, 11680-11688

[14.] D. K. James and M. Tour, "Electrical Measurements in Molecular Electronics," *Chem. Mater.* 2004, vol. 16, 4423 - 4435

[15.] W. Haiss, H. van Zalinge, D. Bethell, J. Ulstrup, D. J. Schiffrin, R. J. Nichols. "Thermal gating of the simgle molecule conductance of alkanedithiols," *Faraday Discussions*, 2005, 131/19 DOI: 10.1039/b507520n

[16.] M. Dorogi, J. Gomez, R. Osifchin, R. P. Andres and R. Reifenberger, "Room temperature coulomb blockade from a self assembled molecular nanostructure," *Phys. Rev. B*, vol. 52, 1995, pp 9071 - 9077

[17.] D.J. Wold, C.D. Frisbie. "Formation of metal-molecule-metal tunnel junctions: Microcontacts to alkanethiol monolayers with a conducting AFP tip," *J. Am. Chem.* Soc. 2000, 122, 2970 - 2971

[18.] X.D. Cui, A. Primak, X. Zarate, J. Tomfhor, O.F. Stanley, A.L. Moore, D. Gust, G. Harris and S.M. Lindsay, "Reproducible measurement of single molecule conductivity," *Science*, 2001, vol. 294, pp 571 - 574

[19.] X.D. Cui, X. Zarate, J. Tomfhor, O.F. Stanley, A. Primak, A.L. Moore, T.A. Moore, D. Gust, G. Harris and S.M. Lindsay, "Making electrical contacts to molecular monolayers," *Nanotechnology*, 2002, vol. 13, pp 5 - 14

[20.] A.S. Blum, J.C. Yang, R. Shashidhar and B. Ratna, "Comparing the conductivity of molecular wires with the scanning tunnelling microscope," *Applied Physics Letters*, 2003, vol. 82, number 19.

[21.] A.M. Rawlett, T.J. Hopson, L.A. Nagahara and R.K. Tsui, "Electrical measurements of a dithiolated electronic molecule via conducting atomic force microscopy," *Applied Physics Letters*, 2002, vol 81, number 16.

[22] C.J. Muller, B.J. Vleeming, M.A. Reed, J.J.S. Lamba, R. Hara, L. Jones II and J.M.Tour, "Atomic probes: A search for conduction through a single molecue," *Nanotechnology*, 1996, vol. 7, pp 409 – 411.

[23] M.A. Reed, C. Zhou, C.J. Muller, T.P. Burgin and J.M. Tour, "Conductance of a molecular junction," *Science*, 1997, vol. 278, pp 252 – 254.

[24] C. Kergueris, J.P. Bourgoin, S. Palacin, D. Esteve, C. Urbina, M. Magoga and C. Joachim, "Electron transport through a metal-molecule-metal junction," *Phys. Rev. B*, 1999, vol. 59, pp 12505 – 12513.

[25] J. Chen, M.A. Reed, A.M. Rawlett and J.M. Tour, "Large on-off ratios and negative differential resistance in a molecular electronic device," *Science*, 1999, vol. 286, pp 1550 -1552.

[26] J.M. Seminario, A.G. Zacarias and J.M. Tour, "Theoretical study of a molecular resonant tunnelling diode," *J. Amer. Chem. Soc*, 2000, vol. 122, pp 3015 – 3020.

[27] J.M. Tour, A.M. Rawlett, M. Kozaki, Y. Yao, R.C. Jagessar, S.M.Dirk, D.W. Price, M.A.Reed, C. Zhou, J. Chen, W. Wang, I. Campbell, "Synthesis and preliminary testing of molecular wires and devices," *Chem. Eur. J*, 2001, vol. 7, num. 23

[28] J.K.N. Mbindyo, T.E. Mallouk, J.B.Mattzela, I. Kratochvilova, B. Razavi, T.N. Jackson and T.S. Mayer, "Template synthesis of metal nanowires containing monolayer molecular junctions," *J. Am. Chem. Soc.* 2002, vol. 124, pp 4020 – 4026.

[29] I. Kratochvilova, M. Kocirik, A. Zambova, J. Mbindyo, T.E. Mallouke and T.S. Mayer, "Room temperature negative differential resistance in molecular nanowires," *J. Mater. Chem.* 2002, vol 12,pp 2927 - 2930

[30] R. L. McCreery, "Molecular Electronic Junctions," *Chem Mater*, 2004, vol 16, pp 4477-4496

[31] J. G. Simmons, "Generalized formula for the electric tunnel effect between similar electrodes separated by a thin insulating film." *Journal of Applied Physics*, vol 34, number 6, June 1963.

[32] Porter M. D, Bright T. B, Allara D. L, Chidseyi C. E. D. "Spontaneously Organized Molecular Assemblies Structural Characterization of n-Alkyl Thiol Monolayers on Gold by Optical Ellipsometry, Infrared Spectroscopy, and Electrochemistry" *J. Am. Chem. Soc.* 1987, vol 109, pp 3559 – 3568

[33]. Hee-Won Seo, Chang-Soo Han, Dae-Geun Choi, Keun-Soo Kim, Young-Hee Lee, Controlled assembly of SWNT bundle using dielectrophoresis, *Microelectronic Engineering*, vol 81, pp83-89, 2005

[34]. Dimaki M, Boggild P, Frequency dependence of the structure and electrical behaviour of carbon nanotube networks assembled by dielectrophoresis, *Nanotechnology*, vol 16, pp759-763, 2005

[35]. Weisman R B, Carbon nanotubes: four degrees of separation, *Nature Materials*, vol 2, pp-569-570, Sept 2003.

[36]. Suehiro J, Zhou G, Imakiire H, Ding W, Hara M, Controlled fabrication of a carbon nanotube NO_2 sensor using dielectrophoretic impedance measurement, *Sensors and Actuators B*, vol 108, pp 398-403, 2005.

[37]. Kaneto K, Tsuruta M, Sakai G, Cho W Y, Ando Y, Electrical Conductivities of multi-wall carbon nanotubes, *Synthetic Metals*, vol 103, pp2543-2546, 1999

[38]. Brown E, Hao L, Gallop J C, Ballistic thermal and electrical conductance measurements on individual multiwall carbon nanotubes, *Applied Physics Letters*, vol 87, 2005

[39]. Jones T.B. Electromechanics of Particles, Cambridge University Press, ISBN 0-521-01910-9

[40]. Nakayama Y, Akita S, Nanoengineering of carbon nanotubes for nanotools, *New Journal of Physics*, vol 5, pp 128.1 – 128.23, 2003

[41]. Dimaki M, Boggild P, Dielectrophoresis of carbon nanotubes using microelectrodes: A numerical study, *Nanotechnology*, vol 15, pp1095 – 1102, 2004

[42]. Bonard J M, Stora T, Salvetat J P, Maier F, Stockli T, Duschl C, Forro L, de Heer W A, Chatelain A, Purification and size selection of carbon nanotubes, *Adv. Mater.* Vol 9 (10), pp827, 1997.

[43]. Bahr J L, Mickelson E T, Bronikowski M J, Smalley R E, Tour J M, Dissolution of small diameter single walled carbon nanotubes in organic solvents? *Chem Commun*, pp 193-194, 2001

[44]. Morgan, H. Green, N. AC Electrokinetics: Colloids and Nanoparticles, Research Studies Press, ISBN 0-86380-255-9

[45]. Giner V, Sancho M, Lee R S, Martinez G, Pethig R, Transverse dipolar chaining in binary suspensions induced by rf fields, J. *Phys. D: Appl. Phys.* vol 32 pp 1182-1186, 1999